Hydrogenation of L-arabinose, D-galactose, D-maltose and L-rhamnose

Víctor Alberto Sifontes Herrera

Laboratory of Industrial Chemistry and Reaction Engineering
Process Chemistry Centre
Department of Chemical Engineering
Åbo Akademi University
Åbo 2012

Víctor Alberto Sifontes Herrera
born in Caracas, Venezuela

M.Sc. (Chem. Eng.) 2006
Simón Bolívar University
Caracas, Venezuela

Hydrogenation of L-arabinose, D-galactose, D-maltose and L-rhamnose

Víctor Alberto Sifontes Herrera

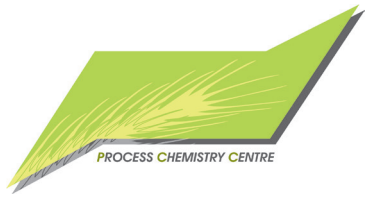

Laboratory of Industrial Chemistry and Reaction Engineering
Process Chemistry Centre
Department of Chemical Engineering
Åbo Akademi University

2012

Supervised by

Academy Professor Tapio O. Salmi
Laboratory of Industrial Chemistry and Reaction Engineering
Process Chemistry Centre
Åbo Akademi University
Åbo/Turku, Finland

and

Professor Dmitry Yu. Murzin
Laboratory of Industrial Chemistry and Reaction Engineering
Process Chemistry Centre
Åbo Akademi University
Åbo/Turku, Finland

ISBN 978-952-12-2731-8
Painosalama Oy – Turku/Åbo, Finland 2012

A quien pueda interesar

PREFACE

The present work was carried out at the Laboratory of Industrial Chemistry and Reaction Engineering, Department of Chemical Engineering at Åbo Akademi University between 2007 and 2012. The research is part of the activities performed at Åbo Akademi Process Chemistry Centre within the Finnish Centre of Excellence Program (2000-2011) by the Academy of Finland. The financial support from the Finnish Graduate School in Chemical Engineering (GSCE) is greatly acknowledged.

Academy Professor Tapio Salmi's deep insights and clever ideas were then, and are still, sincerely appreciated – *tack för Er tillit och Ert tålamod: det händer ju sällan att man hittar en människa med både lysande hjärna och förstående hjärta*. Professor Dmitry Yu. Murzin with his extensive experience, his shrewd sense of comprehension, and an innate passion for teaching and passing on knowledge, *большое спасибо!* And even though it has been stated countless times in the past, I would still like to have my say at how the Laboratory is indeed fortunate to count with such a perfect blend of talent, innovation and expertise.

Top research without wit is unachievable and, thus, for keeping matters clear and the wheels smoothly turning, it is with respect that I would like to express my gratitude to Lab. Dr. Manager Kari Eränen. In the same spirit, Professor Johan Wärnå's understanding of numeric calculation tools has always been opportune, making converge what was not wrong.

My friends have definitely collaborated, in one way or another, to the pursuit and accomplishment of this humble task. *Heidi, Oli – tack för att vi tillsammans låtit oss erfara både vår vänskap och otaliga äventyrer*. The *Merlucillas* have a very special place in the fondest of my memories: Àngela, Betiana, Jean-Noël and Serap, *merci, gracias, gràciets, teşekkürler!* Pierlusconi: *grazie mille* for the requested and unrequested positivity!

Y para finalizar, quisiera darles las gracias a todos aquellos quienes, incluso desde antes del principio, me brindaron su constante apoyo: David, Marianna, César, Juan Carlos, Irene, Paul: es un privilegio contar con amigos como ustedes y que ustedes cuenten también conmigo, obvio. José Rafael y Odette – gracias por todos esos momentos mágicos que compartimos juntos: las tertulias, los conciertos y lo que vendrá.

A mi madre por su inagotable paciencia, por su radiante humor, por sus deliciosas tortas y, sobre todo, por su amor incondicional.

Juhalle – kiitos!

Åbo, January 31st, 2012.

Víctor.

ABSTRACT

Hydrogenation of L-arabinose, D-galactose, D-maltose and L-rhamnose

Keywords: hydrogenation, L-arabinose, D-galactose, D-maltose, L-rhamnose, ruthenium, structured catalysts, ultrasound, sugar mixtures, kinetics, modeling.

In recent years, exploitation of renewable resources has gained considerable attention. Carbohydrates constitute an important fraction of the available renewable biomass and are therefore becoming a key target in the field of green chemistry. A particularly interesting group of molecules derived from carbohydrates are sugar alcohols, which are versatile molecules with a variety of uses, such as low-caloric sweeteners.

The research presented herein encompasses the hydrogenation of D-maltose, D-galactose, L-rhamnose and L-arabinose, which are naturally occurring sugar molecules. The foundations of this work consisted on hydrogenation experiments, which were carried out on a finely dispersed Ru/activated carbon catalyst (2.5 wt. % Ru) with the objective of studying the formation kinetics of the corresponding polyols. The reactions were performed in a stirred tank reactor at temperatures ranging from 90 to 130 °C and hydrogen pressures from 40 to 60 bar.

Out of these efforts, it was possible to attain sugar conversions up to 100%, with some by-product formation at the harsher operating conditions (specially for the disaccharide D-maltose). Under moderate conditions (temperatures lower than 105 °C) the by-product formation was negligible. The catalyst employed in the study was characterized by scanning electron microcopy (SEM), transmission electron microscopy (TEM), inductively coupled plasma optical emission spectrometry (ICP-OES), and nitrogen physisorption. Rival kinetic models based on the Langmuir-Hinshelwood concepts were proposed for the reactions and a non-linear regression was performed to obtain the numerical values of the kinetic parameters. These models predicted well the sugar hydrogenation process and they can thus be used to design batchwise operating slurry reactors.

To reveal the reaction kinetics and mechanism in more detail, and additional to single-molecule hydrogenations, experiments with synthetically prepared mixtures of L-arabinose and D-galactose (the key components of the hemicellulose

arabinogalactan) were carried out at different temperatures (90, 105 and 120 °C) and pressures (40, 50 and 60 bar of hydrogen) at diverse galactose-to-arabinose ratios (from 0.1 to 10), using the same Ru/C catalyst as before.

Complete conversions were achieved with excellent selectivities exceeding 95% and without any unexpected effects of temperature and pressure. The assumption of competitive adsorption for the simultaneous reduction of both sugar molecules provided a detailed kinetic model that was able to describe the results very well.

In order to seek intensification routes that would render the production of sugar alcohols even more effective, a study on the impact of ultrasound on the hydrogenation of L-arabinose and D-galactose was undertaken. These experiments were carried out with the typical Ru/active carbon catalyst at 105 °C and 50 bar of hydrogen. Three methods of acoustic irradiation were applied (direct and indirect on-line irradiation and catalyst pre-treatment with ultrasound). The irradiation power was studied in the case of indirect irradiation and the effects of pressure and concentration were investigated. The characterization of fresh and spent catalyst was carried out by N_2 physisorption, TEM, and SEM.

It emerged that the ultrasound effect turned out to be independent of both the concentration of sugar and the hydrogen pressure, and that it can, in some cases (D-galactose), enhance the hydrogenation rate on the Ru/C catalyst but it cannot, however, prevent the catalyst deactivation. A kinetic model for the deactivation was developed.

The next step consisted in the measurement of the density, viscosity and hydrogen solubility of the aqueous solutions of the sugar molecules. NMR studies of the molecules were also performed. The physical properties of sugar solutions were used to estimate the liquid-phase diffusion coefficients, which were then incorporated into a reaction-diffusion-catalyst deactivation model for porous catalyst layers. The model indicated that diffusional resistance becomes severe for rather small catalyst particles ($\geq$ 1 mm), which suggests that structured reactors would provide a better approach than the conventional fixed bed technology, if continuous operation is desired.

Following these results, continuous hydrogenation of L-arabinose was carried out with ruthenium on three different supports (active carbon clothes, carbon

nanotubes on sponge-like metallic structures, and crushed commercial active carbon extrudates). It was demonstrated that it is possible to convert sugars (L-arabinose) to their corresponding sugar alcohol (L-arabitol) with very high selectivities using a Ru/Active carbon cloth as a catalyst.

From batch to continuous processes, it was demonstrated with this body of work that hydrogenation of the selected sugar molecules (L-arabinose, D-galactose, D-maltose and L-rhamnose) is a fully feasible process route for obtaining fine chemicals that can, in addition, be materialized in a larger scale.

REFERAT

Hydrering av L-arabinos, D-galaktos, D-maltos och L-ramnos

Nyckelord: hydrering, L-arabinos, D-galaktos, D-maltos, L-ramnos, rutenium, strukturerade katalysatorer, ultraljud, sockerblandningar, kinetik, modellering.

Under de senaste åren har intresset för utnyttjandet av förnybara resurser kraftigt ökat. I samband med detta utgör kolhydrater en viktig del av den tillgängliga förnybara biomassan och den har därefter blivit föremål för ett stort intresse inom hållbar kemi. Sockeralkoholer är en särskilt viktig grupp av molekyler som vanligtvis erhålls ur kolhydrater och som har mångsidiga tillämpningar som t.ex. lågkalorihaltiga sötningsmedel.

Häri presenterade forskningen omfattar hydreringen av naturligt förekommande sockerarter L-arabinos, D-galaktos, D-maltos och L-ramnos. Grunden för detta arbete består av hydreringsexperiment som utfördes på en dispergerad Ru/aktiv kolkatalysator (2.5 %vikt Ru) i syfte att studera bildningskinetiken av de motsvarande sockeralkoholerna. Reaktionerna genomfördes i en omrörd satsvis laboratoriereaktor vid temperaturer mellan 90 och 130 °C och vätetryck mellan 40 och 60 bar.

Under dessa betingelser var det möjligt att åstadkomma sockeromvandlingar upp till 100 % med en viss biproduktbildning vid kraftigare processbetingelser (särskilt i hydrering av D-maltos). Bildningen av biprodukter var dock försumbar under måttliga betingelser (temperaturer lägre än 105 °C). Den katalysator som användes i forskningen karakteriserades med svepelektronmikroskopi (SEM), transmissionselektronmikroskopi (TEM), optisk emissionsspektrometri med induktivt kopplad plasma (ICP-OES) samt fysisorption av kväve. Konkurrerande kinetiska modeller som baserades på Langmuir-Hinshelwood-konceptet föreslogs för att beskriva reaktionerna. Parametrar i hastighetsekvationerna bestämdes därefter genom icke-linjär regression. Dessa modeller kunde väl förutsäga hydreringsreaktionernas förlopp och de kan följaktligen användas för design av omrörda satsreaktorer.

Ytterligare hydreringsexperiment med sockerblandningar (istället för isolerade molekyler) genomfördes för att fördjupa kunskaper i kinetik och reaktionsmekanismer av sockerhydreringen. Studierna genomfördes med syntetiska socker-

blandningar av L-arabinos och D-galaktos (de viktigaste komponenterna i hemicellulosan arabinogalaktan) vid olika temperaturer (90, 105 och 120 °C) och vätetryck (40, 50 och 60 bar). Förhållanden mellan D-galaktos och L-arabinos i blandningarna varierades mellan 0,1 och 10 och samma Ru/C katalysator som i tidigare experiment användes.

Fullständig omsättning uppnåddes med utmärkta selektiviteter som överskred 95 % och dessutom inverkade varken temperatur eller vätetryck på reaktionens förlopp på något oväntat sätt. Antagandet av konkurrerande adsorption för en samtidig reduktion av båda sockermolekylerna gav en kinetisk modell som noggrant beskrev de experimentella resultaten.

Idén om att utforska potentiella sätt att påskynda bildningen av sockeralkoholer ledde till utföringen av hydreringsexperiment med L-arabinos och D-galaktos i närvaro av ultraljud. Dessa experiment genomfördes med den redan sedvanliga Ru/C-katalysatorn vid 105 °C och 50 bar väte. Tre olika metoder för ultraljudsbestrålning tillämpades (direkt och indirekt on-line-bestrålning samt akustisk förbehandling av katalysatorn). Strålningens effekt mättes vid den indirekta tillämpningen samt inverkan av temperaturen och trycket. Katalysatorn karakteriserades i färsk och förbrukad form genom fysisorption av kväve, TEM och SEM.

Det visade sig att ultraljudets inverkan var oberoende av sockerhalten och vätetrycket och att bestrålningen gynnade hydreringen av D-galaktos trots att den inte förhindrade Ru/C-katalysatorns deaktivering överhuvudtaget. En kinetisk modell som beaktade deaktiveringen utvecklades.

Sockerlösningarnas densitet, viskositet och vätelöslighet uppmättes och modellerades. NMR-spektroskopi användes för att studera sockermolekylernas jämvikter i vattenlösningar. Sockerlösningarnas fysikaliska egenskaper användes för att beräkna diffusionskoefficienter, som i sin tur infogades i en modell för kopplad diffusion, reaktion och katalysatordeaktivering hos porösa katalytiska skikt. Modellen avslöjade att diffusionsmotståndet dramatiskt förstärks redan för ganska små katalysatorpartiklar (< 1 mm), vilket tyder på att strukturella reaktorer är överlägsna de konventionella fastbäddreaktorerna, ifall kontinuerlig drift önskas.

Dessa undersökningar följdes av kontinuerlig hydrering av L-arabinos med tre olika Ru-katalysatorer på tre olika bärare: tyg av aktivt kol, kolnanorör på svampliknande metalliska strukturer samt krossade partiklar av en kommersiell

Ru/C-katalysator. Det visade sig att det var möjligt att omvandla L-arabinos till arabitol med höga selektiviteter med hjälp av Ru/koltyg-katalysatorn.

Från satsvis drift till kontinuerliga processer: genom dessa insatser demonstrerades att hydreringen av de valda sockerarterna är en helt genomförbar rutt till framställning av fin- och specialkemikalier, som dessutom kan förverkligas i större skala.

RESUMEN

Hidrogenación de L-arabinosa, D-galactosa, D-maltosa y L-ramnosa

Palabras claves: hidrogenación, L-arabinosa, D-galactosa, D-maltosa, L-ramnosa, rutenio, catalizadores estructurados, ultrasonido, mezclas de azúcares, cinética, modelado.

La explotación de recursos renovables ha ganado recientemente atención considerable. Los carbohidratos, que constituyen parte importante de la biomasa renovable disponible, han sido objeto de gran interés en el campo de la química sustentable. De estos se derivan los polialcoholes, un grupo de moléculas particularmente interesantes, las cuales cuentan con una variedad de aplicaciones tales como edulcorantes de bajo contenido energético.

El cuerpo de investigación contenido en estas páginas trata sobre la hidrogenación de L-arabinosa, D-galactosa, D-maltosa y L-ramnosa, monosacáridos de origen natural. Los cimientos de este trabajo los constituyen experimentos de hidrogenación asistida por un catalizador de rutenio (2,5 %peso Ru) finamente disperso, los cuales se efectuaron con el fin de estudiar la cinética de formación de los polialcoholes pertinentes. Las reacciones se llevaron a cabo a temperaturas entre los 90 y los 130 °C y a presiones de hidrógeno entre los 40 y 60 bar.

Gracias a estos esfuerzos fue posible obtener conversiones de hasta un 100% con cierta formación de productos secundarios en el caso de las condiciones operacionales más extremas (especialmente evidente en la hidrogenación de D-maltosa). Bajo condiciones moderadas (temperaturas por debajo de los 105 °C), la formación de productos secundarios resultó insignificante. Los catalizadores empleados en este estudio fueron caracterizados por microscopía electrónica de barrido, microscopía electrónica de transmisión y espectroscopía de emisión óptica con fuente de plasma de acoplamiento inductivo, abreviadas SEM, TEM e ICP-OES respectivamente por sus siglas en inglés, además de adsorción física de nitrógeno. Se propusieron además diversos modelos cinéticos basados en la teoría de Langmuir-Hinshelwood, cuyos parámetros se obtuvieron mediante regresión numérica no-lineal. Estos modelos fueron capaces de describir correctamente las reacciones de hidrogenación y, por ende, son aptos para diseñar reactores no-estacionarios tipo tanque agitado.

Además de experimentar con los azúcares por separado, también se llevaron a cabo experimentos con mezclas sintéticas preparadas a partir de L-arabinosa y D-galactosa (ambos componentes clave del arabinogalactano, una hemicelulosa) lo cual permitió profundizar en el mecanismo y cinética de reacción. Dichos experimentos se realizaron a temperaturas de 90, 105 y 120 °C y presiones de hidrógeno de 40, 50 y 60 bar con los azúcares presentes en diferentes relaciones de mezcla de galactosa a arabinosa (entre 0,1 y 10), manteniendo siempre el catalizador de rutenio utilizado en los estudios anteriores.

Se obtuvieron conversiones totales con una excelente selectividad superior al 95 % y sin observar efectos imprevistos de presión o temperatura. La suposición de una adsorción competitiva dio como resultado un modelo cinético capaz de describir con exactitud la reducción simultánea de ambos azúcares.

Con el objeto de hacer aún más eficiente la producción de polialcoholes, se estudió el impacto del ultrasonido en la hidrogenación de L-arabinosa y D-galactosa. Estos experimentos fueron realizados con el catalizador de rutenio habitual a 150 °C de temperatura y 50 bar de hidrógeno. Tres métodos diferentes de irradiación ultrasónica fueron utilizados (irradiación directa e indirecta y pre-tratamiento del catalizador con ultrasonido). Los efectos de presión y temperatura en la tasa de reacción fueron investigados y la potencia de irradiación fue evaluada en el caso de irradiación indirecta. Tanto el catalizador fresco como el usado fueron caracterizados mediante SEM, TEM y adsorción de nitrógeno.

Se constató que el efecto del ultrasonido es independiente de la presión y de la concentración de azúcar y que, en el caso de D-galactosa, favorece la reacción de hidrogenación. Sin embargo, la implementación del ultrasonido no ayudó a prevenir la desactivación del catalizador. Finalmente, se propuso un modelo cinético que toma en cuenta el efecto de la desactivación.

A continuación, se procedió a determinar la densidad, la viscosidad y la solubilidad de hidrógeno en soluciones acuosas de azúcar. Asimismo, se realizaron estudios de espectroscopía de resonancia magnética nuclear (RMN). Las propiedades físicas estudiadas permitieron estimar los coeficientes de difusión en fase líquida, los cuales fueron incorporados en un modelo de difusión, reacción y desactivación para catalizadores porosos. Con este modelo se logró demostrar que la resistencia a la transferencia de masa se agrava en partículas de catalizador relativamente pequeñas (≥ 1 mm), lo cual sugiere que, de apuntar a una opera-

ción continua, los reactores estructurados son una alternativa potencialmente superior a la tecnología convencional de reactores de lecho fijo.

Siguiendo estas recomendaciones, se inició el estudio de la hidrogenación continua de L-arabinosa. Para ello se dispuso de tres catalizadores de rutenio depositado en tres soportes diferentes: tejidos de carbón activado, esponjas metálicas cubiertas con nanotubos de carbón, y partículas finamente trituradas de un catalizador comercial a base de carbón activado. La mayor conversión, con una alta selectividad para con L-arabitol, se obtuvo mediante la utilización del catalizador de rutenio depositado en tejidos de carbón activado.

Para concluir, es posible afirmar que con este trabajo queda demostrado que la hidrogenación de los azúcares seleccionados (L-arabinosa, D-galactosa, D-maltosa y L-ramnosa) es un proceso totalmente viable, tanto en reactores por lotes como continuos, para la obtención de productos químicos de valor agregado que puede ser incluso trasladado a escala industrial.

LIST OF PUBLICATIONS

I. Sifontes Herrera, V. A., Oladele, O., Kordás, K., Eränen, K., Mikkola, J.-P., Murzin, D. Y., & Salmi, T. (2011). Sugar hydrogenation over a Ru/C catalyst. *Journal of Chemical Technology & Biotechnology*, *86*(5), 658-668. doi:10.1002/jctb.2565

II. Sifontes Herrera, V.A., Saleem, F., Kusema, B., Eränen, K., & Salmi, T. Hydrogenation of L-arabinose and D-galactose mixtures over a heterogeneous Ru/C catalyst. *Industrial and Engineering Chemistry Research (submitted)*.

III. Sifontes Herrera, V.A., Tourvieille, J.-N., Leino, A.-R., Eränen, K., & Salmi, T. Ultrasound effect on hydrogenation of sugars: catalyst deactivation and modeling. *Applied catalysis (submitted)*.

IV. Sifontes, V. A., Rivero, D., Wärnå, J.P., Mikkola, J.-P., & Salmi, T. O. (2010). Sugar Hydrogenation Over Supported Ru/C — Kinetics and Physical Properties. *Topics in Catalysis*, *53*(15-18), 1278-1281. Springer Netherlands. doi:10.1007/s11244-010-9582-9.

V. Sifontes Herrera, V.A., Rivero Mendoza, D.E., Leino, A.-R., Mikkola, J.-P., Zolotukhin, A., Eränen, K., & Salmi, T. Sugar hydrogenation in continuous reactors: from catalyst particles towards structured catalysts. *Chemical Engineering and Processing: Process Intensification (submitted)*.

LIST OF CONFERENCE PRESENTATIONS

- V. A. Sifontes Herrera, O. Oladele, K. Kordás, K. Eränen, D. Yu. Murzin, and T. Salmi, *Sugar hydrogenation for the production of alternative sweeteners*. INNOVATION III - COST-D40 Action in Innovative Catalysis: New Processes and Selectivities. May 26 – 28, 2009, Turku, Finland. (Poster presentation)
- V. A. Sifontes Herrera, O. Oladele, K. Kordás, K. Eränen, D. Yu. Murzin, and T. Salmi. *Sugar hydrogenation for the production of alternative sweeteners.* 8th World Congress of Chemical Engineering. August 23 – 27, 2009, Montréal, Canada. (Poster presentation)
- T.Salmi, J. Kuusisto, V. Sifontes, J. Wärnå, D. Rivero. *Sugar hydrogenation on Ru/C – slurry, fixed bed and monoliths*. 3rd International Conference on Structured Catalysts And Reactors. September 27-30, 2009 Ischia, Italy. (Oral presentation)
- J. Wärnå, T. Salmi, J. Kuusisto, V. Sifontes, D. Rivero, J.-P. Mikkola. *Interaction of reaction, diffusion and catalyst deactivation in sugar hydrogenation.* International Symposium on Catalyst Deactivation. October 25 - 28, 2009, Delft, the Netherlands. (Poster presenation)
- V. Sifontes, D. Rivero, J. Wärnå, J.-P. Mikkola, T. Salmi. *Sugar Hydrogenation over supported Ru/C – Kinetics and Physical Properties*. 23rd Organic Reactions Catalysis Society Conference. March 14-18, 2010, Monterey, California, USA. (Poster and Oral presentation).
- V. Sifontes, F. Saleem, B. Kusema, T. Salmi. *Hydrogenation of L-arabinose and D-galactose mixtures over heterogenous Ru/C catalyst*. 24rd Organic Reactions Catalysis Society Conference. April 15-19, 2012, Annapolis, Maryland, USA. (Poster presentation).

TABLE OF CONTENTS

1 Introduction

1.1 General

Over the last decade, the deep dependence on fossil feedstock has become a source of preoccupations for industries, politicians and environmentalists alike, thus highlighting the need of a move towards renewable raw materials. In this sense, biomass has been profiled as the keystone of a fossil-free industry: renewable, energy rich and CO_2-neutral. Biomass is an abundant and rich source of molecules, which can be further refined to yield diverse chemicals, food ingredients and fuels. However, an efficient use of these resources implies that all the potential within each synthesis route leading to a given biomass derivative should rely as little as possible on external sources (e.g., fossil feedstock) and profit the varied functionality that constitutes the core components of biomass.

Nonetheless, the current state at which biomass energetic and chemical capacities are being exploited still needs to be developed. Moreover, a key for a successful transition towards an economy based on renewables depends on diversification[1], implying that not only the energetic fractions (e.g., biofuels, direct combustion, etc.) of the feedstock should be taken advantage of.

However, it should not be ignored that the key target for substitution by biomass derivatives are fossil fuels, as not only the lighter, and thus cheaper, sources of oil are running dry but the fossil reservoirs as a whole will not last forever, while paradoxically the need for fuels and energy, in general, is steadily mounting. To meet this problem, the use of fuels derived from biomass has been proposed[2]. While it is beyond the scope of this work to give a full account on biorefinery and biofuels, it is important to highlight that such a platform has been a coveted topic during the past years. The so-called first generation biofuels relies mostly on sugar monomers derived from edible crops for the production bioethanol. While environmentally friendly, the competition for cultivable land and the high production cost hinder, at the present time, the broader implementation of this technology.

Then came the second generation of biofuels, which sought to address the issue by focusing instead on waste streams stemming from the paper and agricultural industries, among other sources. This implies the less straightforward task of refining and adding value to complex molecules such as cellulose, hemicelluloses, and lignin. The driving force of this technology lies in its very own complexity: long chains of highly functionalized molecules. From here, many processes have been envisioned, with the platform based on levulinic acid derived from glucose for the production of hydrocarbons having garnered considerable attention lately.[2,3]

Interestingly enough, not only fuels can be obtained from biomass, as platforms based on carbohydrates for the production of specialty and fine chemicals have already been proposed: one example being polyesters, polyamides and polyurethane derived from sorbitol, which in turn is obtained from glucose, the building block of starches and cellulose.[4]

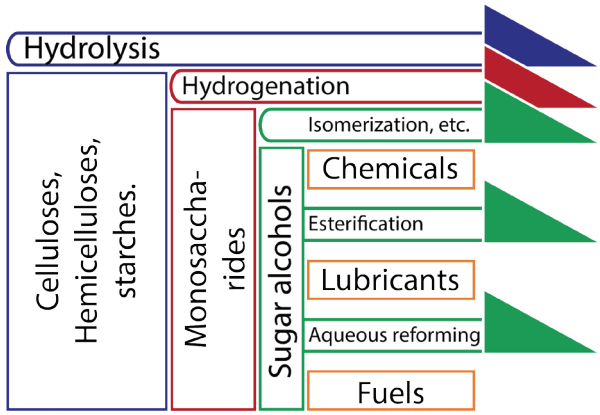

Figure 1.1. Biorefinery scheme.

In this sense, carbohydrates constitute three quarters of the available renewable biomass[5] and they are indeed the building blocks of lignocellulosic biomass. Simpler carbohydrates, such as mono- and disaccharides, are obtained by catalytic hydrolysis of cellulose, hemicelluloses and starch, and their derivatization into useful components is an evident matter. A particularly important route is the hydrogenation of sugars to sugar alcohols. Sugar alcohols, traditionally used as low-caloric sweeteners, have experienced an explosive growth in interest, due not only to their potential as platform molecules as mentioned above, but also due to their role in aqueous-phase reforming, which has been envisioned as a route to renewable hydrogen by exposing aqueous solutions of oxygenated hy-

drocarbons, e.g. sorbitol, to temperatures above 500 K and, depending on the desired selectivity towards H_2, a Pt-catalyst.[6]

However, not only should the naturally occurring carbohydrates become an important part of the industrial feedstock but also, in order to guarantee a smooth transition to a biomass-based industry, the products derived thereof should be developed having the alternative raw materials in mind, as opposed to seeking routes to reproduce the exactly same chemicals obtained from other technologies.

In agreement with this strategy, naturally occurring polysaccharides, such as hemicelluloses, are the ideal starting molecules for the derivatization to simpler mono- and disaccharides which, in turn, act as substrates for the production of value added molecules (Figure 1.1).

1.2 Sugars, carbohydrates and monosaccharides

The term *carbohydrate* was in the beginning used only to refer to molecules whose constitution was made up of carbon, hydrogen and oxygen in the proportions $C_n(H_2O)_n$. However, due to the functional richness of such compounds, which range from the fundamental monosaccharides to highly substituted molecules, the term has lost its specificity. On the other hand, the word *sugar* is mainly used to describe monosaccharides and simpler oligosaccharides, such as glucose and sucrose (table sugar)[7,8]

Finally, *monosaccharide* refers to the most basic molecules that constitute the building blocs of more complex carbohydrates. Generally, a monosaccharide will contain several hydroxyl groups and a carbonyl function. The terms *aldose* and *ketose* refer to those monosaccharides whose carbonyl function is an aldehyde or a ketone, respectively.

Besides the number of carbons, the number of hydroxyl groups and the type of the carbonyl function present in monosaccharides and, more generally, in carbohydrates, other factors should also be considered when studying these compounds. Due to the presence of hydroxyl and carbonyl groups on the same carbon chain, intramolecular hemiacetal formation takes place. The result of these internal reactions is the co-existence of a particular carbohydrate molecule in five-membered rings (furanoses) or six-membered rings (pyranoses), with other

cyclic configurations being also possible but uncommon as the strong torsion inside the molecule renders it less stable. Finally, the ring closure at the planar carbonyl group can take place from either side, which gives rise to the α and β anomers. Besides the cyclic forms, minor fractions of the molecules exist in open-chain forms, in which the carbonyl group is presumed to be active.

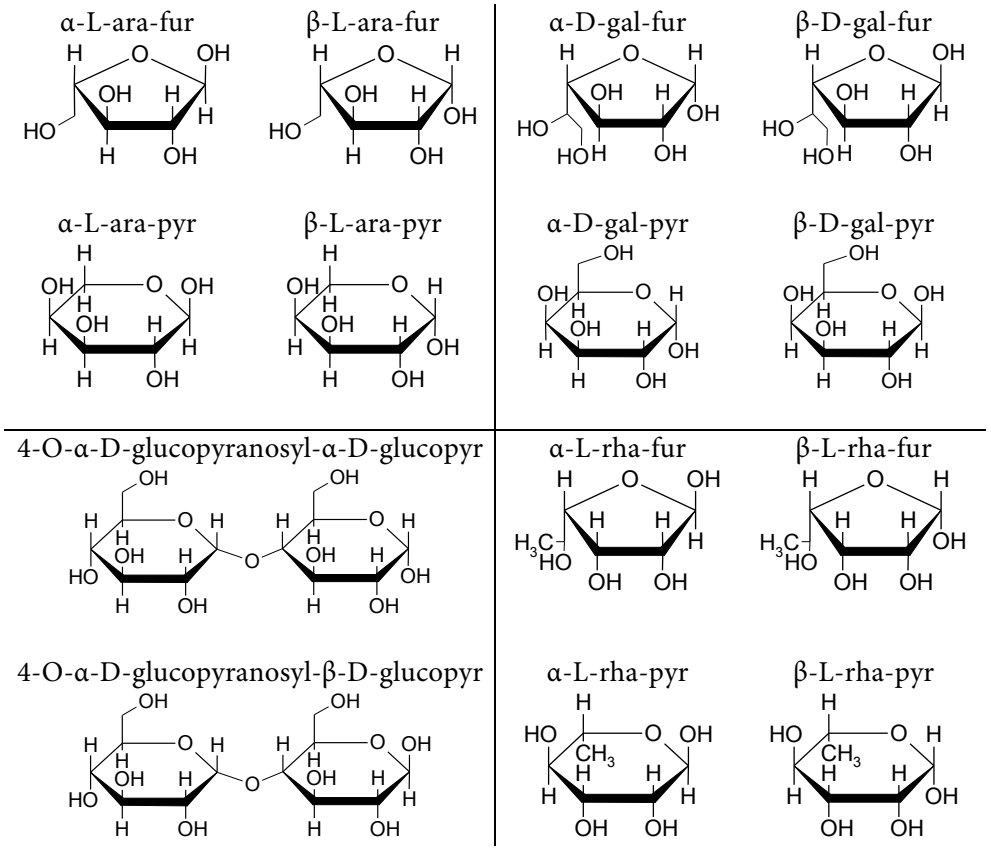

Figure 1.2. Studied molecules. Upper left: L-arabinose, upper right: D-galactose, lower left: D-maltose, lower right: L-rhamnose. Pyr = pyranose, fur = furanose. Ara = arabinose, gal = galactose, rha = rhamnose.

Nonetheless, being complex molecules as they are, it follows that a thorough presentation of the classification of carbohydrates goes well beyond the purposes of this work. The concerned reader is consequently advised to consult the literature.[8,9]

The molecules relevant to this work are L-arabinose, D-galactose, D-maltose and L-rhamnose, which are presented Figure 1.2 in their four most common tautomeric forms.

1.3 Sugar alcohols

Sugar alcohols, known also as polyols or alditols, are compounds obtained through the reduction of the carbonyl group present in a sugar molecule either by means of chemical agents (such as sodium borohydride) or by molecular hydrogen in the presence of a homogeneous or heterogeneous catalyst. The catalytic route is preferred in the industrial hydrogenation of sugars into sugar alcohols, where heterogeneous catalysts based on Ni, Pd, Pt or Ru are of choice.[10,11] The use of molecular hydrogen and heterogeneous catalyst is preferred from the viewpoint of green process technology, since the formation of stoichiometric co-products is avoided and the separation of a heterogeneous catalyst from the reaction mixture is rather straightforward. It has been suggested that the reduction reaction occurs by adsorption of the carbonyl group in the open form of the sugar onto the active surface of the catalyst, which further polarizes the carbon and renders it open to a nucleophilic attack by adsorbed hydrogen.[12] The reactions pertinent to the present work are presented in Figure 1.3.

Sugar alcohols are versatile molecules, which have found a wide variety of applications. Higher molecular weight polyols (chains longer than four carbon atoms) could be used for manufacturing polyesters, alkyd resins and polyurethanes.[10] They have also found utilization as intermediates in the production of pharmaceuticals and starting molecules for the synthesis of ligands.[13–20] However, their most commonly known use is connected to the fact that polyols possess a sweet taste, contain fewer calories, and produce a lower glycemic response, thus their use as sweeteners is rather logic.[21,22] As a proof of the evolving importance of this topic, the global production of sorbitol has boosted from 700,000 t/a in 2007[10] to over 1,000,000 t/a in 2009.[23]

1.4 Industrial production of sugar alcohols

Although these reactions are at the core of many important industrial processes, the availability of literature regarding catalytic sugar hydrogenation is relatively scarce. However, work on sugar hydrogenation has been carried out by some

research groups throughout the years, and most of this work has been devoted to the hydrogenation of glucose, fructose, xylose and lactose.[24–30]

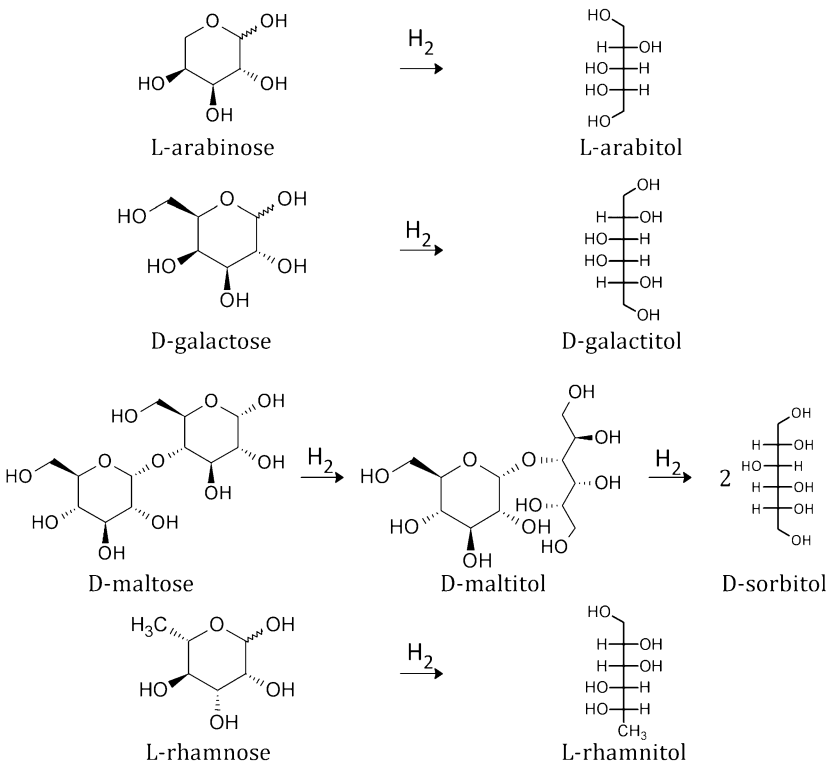

Figure 1.3. Reaction schemes for the hydrogenation to sugar alcohols.

The most common solid catalysts used for sugar hydrogenation to sugar alcohols in industrial scale are based on nickel, such as sponge nickel (Raney nickel), but recently the use of ruthenium has benefited from a growing interest, since Ru has shown a good activity and an excellent selectivity in the hydrogenation of sugar molecules.[10,26,28,31] Thus, it is expected that Ru will replace Ni as a sugar hydrogenation catalyst, particularly because of the toxic properties of Ni (classified as probably carcinogenic by the IARC)[32] the rapid deactivation of Ni and the problematic pyrophoric properties of Raney nickel catalysts.

Typically, the selectivity towards the sugar alcohol is high, both on sponge Ni and Ru catalysts, exceeding 95% under optimal conditions. Such data has been reported for the hydrogenation of glucose, xylose and lactose.[24,28,33–35] For some special cases, such as hydrogenation of fructose to mannitol, the product selec-

tivity is a big issue; the best selectivities of mannitol are limited to about 60 - 70% on Cu-based catalysts, the by-product being sorbitol.[36]

The conventional production technology of sugar alcohols is based on the use of batch-wise operating slurry reactors: finely dispersed, supported or sponge metal catalysts (catalyst particles smaller than 0.1 mm) are immersed in a batch of an aqueous sugar solution, to which hydrogen is continuously added so that the pressure is maintained constant. Among the reported operating conditions, it can be found that the hydrogen pressure is typically kept at 30-180 bar and the temperature ranges from 80 °C to 150 °C.[23,27] The hydrogen concentration in the liquid phase is one of the limiting factors of the process; therefore alternative solvents with better hydrogen solubility, such as ethanol, have been proposed.[34]

In recent years, the continuous operation in sugar hydrogenation has been demonstrated, for instance, for glucose hydrogenation in trickle-bed reactors, monoliths and on activated carbon cloths.[10,11,23] Furthermore, it is possible to carry out sugar hydrogenation in loop reactors, where the sugar solution is recirculated through an external loop system.[23] Since the sugar molecules are large and the solubility of hydrogen is limited, the diffusion limitation inside the porous catalyst layer becomes severe in porous catalyst layers, as has been demonstrated experimentally and by numerical simulations.[37,38] Therefore, only egg-shell catalyst pellets and structured catalysts can be considered as feasible alternatives to slurry technology.

1.5 Ultrasound

Ultrasound, by definition, is the fraction of the sonic spectrum with frequencies higher than 20 KHz, above the threshold of human hearing. It has a wide range of general applications, such as medical diagnostic sonography, cleaning, dissolving, or initiating the reaction in biological, chemical and electrochemical systems. The latter use, incorporation of ultrasonic energy into chemistry, or sonochemistry, has developed into an exciting field of research during the last twenty years. As such, ultrasound has proven to be a very efficient tool in enhancing the reaction rates in a variety of reacting systems (e.g. reactions on Ni[39]), but also in improving the selectivity and activity of heterogeneous catalytic reactions.[40–43]

Even though the scale-up of ultrasound technology has been burdened by inefficiency and high operating costs, ultrasound is currently attracting the attention

of the industry, since it might ultimately aid in the reduction of other operating costs: ultrasound may enable reactions under milder conditions (e.g. lower temperatures and pressures), reduce the need for additional costly solvents, and reduce the number of synthesis steps, while simultaneously increasing end yields, making possible the use of lower purity reagents and solvents, and increase the activity of existing catalysts.[43] For these reasons, the use of ultrasound seems to be an interesting technology for the production of added-value chemicals and pharmaceuticals.

In the present work we studied the hydrogenation of L-arabinose and D-galactose on a heterogeneous catalyst (ruthenium on active carbon) in the presence and absence of ultrasound. These sugars occur naturally and they can also be obtained by acid hydrolysis of arabinogalactan polymers (hemicelluloses) naturally appearing in biomass.

1.6 Research strategy

The hydrogenation of L-arabinose, D-galactose, D-maltose and L-rhamnose was studied following the general strategy depicted in Figure 1.4. The starting point of the research was the determination of the intrinsic kinetics of the reduction of the chosen molecules to yield the corresponding sugar alcohols (**Publication I**).

The kinetic studies were carried out in a laboratory-scale slurry batch reactor loaded with a powder Ru/C catalyst. The temperature ranged from 90 to 130 °C and the pressure from 40 to 60 bar. The catalyst particles were small and the stirring speed was high, to suppress internal and external mass transfer resistance. Additionally, the catalyst was characterized. It became already evident at this early stage that the chosen catalyst and operative conditions were ideal for complete conversions with high (>95%) selectivities. Extensive modeling was performed.

In **Publication II**, it was confirmed that sugars in mixtures do also hydrogenate to the corresponding alditols with minimal by-product formation and maximal conversion. The study was performed only on L-arabinose + D-galactose mixtures, as these two monosaccharides form the building blocks of arabinogalactan (a common hemicellulose found in trees). Additional to exploring the temperature (90 to 120 °C) and pressure ranges (40 to 60 bar), the focus was set on the

sugar proportion ratios. The kinetic behavior of the sugar mixtures was modeled mathematically.

Despite the fact that sugar hydrogenation proceeded smoothly and effectively on a Ru/C catalyst and under the aforementioned operating conditions, it became a point of interest to test the effect of ultrasound on these promising reactions. The studied molecules were L-arabinose and D-galactose. As documented in **Publication III**, the effect of either irradiating the reaction medium *in-situ* or pre-treating the catalyst with ultrasound was beneficial only for D-galactose and it proved to be detrimental for L-arabinose. A physical explanation for this was provided.

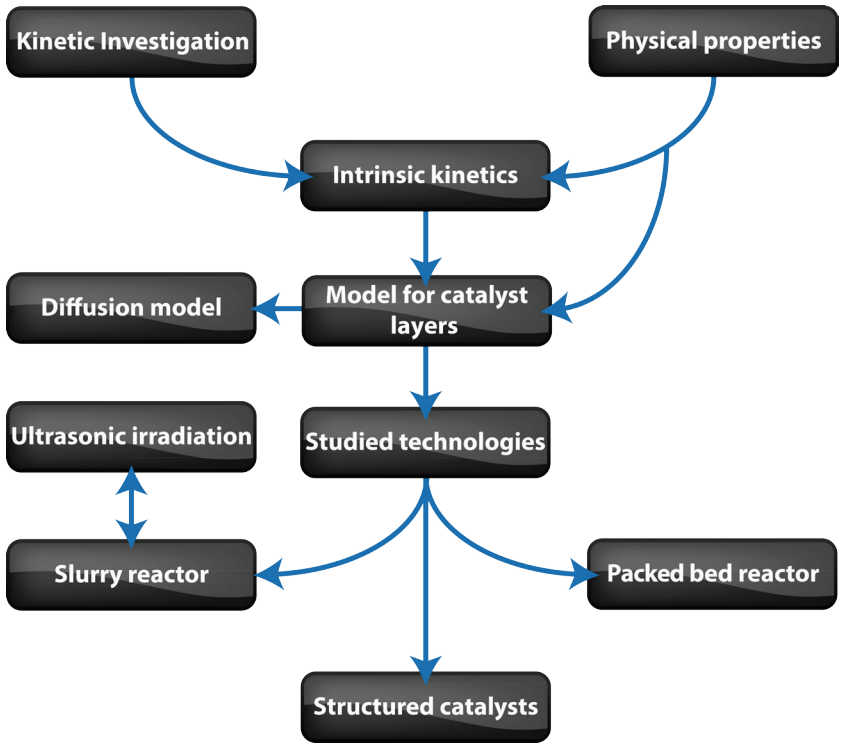

Figure 1.4. Research strategy.

Additional to all the experimental activities, modeling studies were carried out in parallel to the laboratory work. **Publications I-III** include sections devoted to advancing possible mechanisms for the production of sugar alcohols and provide with rate expressions useful for extrapolation of the technology to other reaction schemes, such as continuous reactors. The models provided a good prediction of

the experimental values. **Publication IV** dealt purely with mathematical simulations of sugar hydrogenation and diffusion in catalyst particles. To be able to carry out these calculations, all the previously gathered kinetic knowledge was needed in addition to experimental determination of key physical properties of sugar solutions, namely density, viscosity and hydrogen solubility. The simulation revealed the role of internal diffusion in catalyst particles and gave indications for the design of catalyst structures for large-scale production.

The physical properties are summarized in **Publication V**, together with accounts on implementation of continuous reactors to the hydrogenation of L-arabinose. Synthesis of structural catalysts (carbon on steel structures and active carbon clothes) and fractional factorial screening of operation conditions on more typical trickle bed reactors were reported in **Publication V**.

2 EXPERIMENTAL

2.1 Hydrogenation experiments

2.1.1 Kinetic studies

The hydrogenation reactions were performed in a laboratory-scale batch reactor (Parr 4561, 300 mL) equipped with baffles, a gas entrainment impeller, a sampling line with a sintered filter (7 μm), a cooling coil, a heating jacket, a temperature and stirring rate controller (Parr 4843), a pressure controller and microprocessor (Brooks 5866 and Brooks 0154 respectively), and a bubbling chamber for pre-treating the sugar solutions (Figure 2.1).

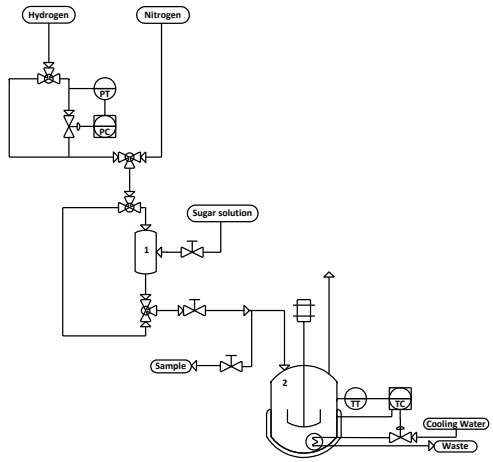

Figure 2.1. Reaction system: (1) bubbling chamber, (2) reaction vessel.

A series of experiments were carried out with the purpose of studying the kinetic behavior of the hydrogenation reactions of four selected sugars (D-maltose, D-galactose, L-arabinose and L-rhamnose; Danisco Sweeteners). For each sugar, a set of experiments was performed at different pressures (40, 50 and 60 bar) and temperatures (90, 105, 120 and 130 °C) in the presence of a supported Ru/active carbon catalyst with a loading of 0.91 wt. % (relative to the dry sugar mass).

The catalyst was loaded in the vessel and flushed with nitrogen (99.999%, AGA) to purge oxygen. At the same time, the sugar was diluted in deionized water. Concentrated solutions are prone to cause mass transport limitation[33], thus it was convenient to work with sugar solutions with concentrations of 10 wt. % and, in the unique case of D-galactose, 4 wt. % (due to the lower solubility of D-galactitol). The sugar solutions were then bubbled with nitrogen and, immediately afterwards, with hydrogen. In the next step, the solution was injected into the vessel, nitrogen was purged with hydrogen, and the system was finally adjusted to the desired operating conditions. Each experiment was carried out at a stirring speed of 1800 rpm for three hours, since it had been previously shown that similar systems required stirring speeds of 1500 – 1600 rpm to ensure operation in the kinetically controlled regime.[24,28,29,44] Samples were withdrawn from the system at different intervals in order to perform the concentration and pH measurements.

In the case of synthetic sugar mixtures, the hydrogenation reactions were also performed on a Ru/C catalyst with sugar solutions of varying molar ratios of D-galactose (Danisco) to L-arabinose (Sigma-Aldrich) in order to study the simultaneous kinetic behavior and interactions of both molecules on the catalyst surface. The procedure was identical to the one described above.

2.1.2 Sugar hydrogenation in the presence of ultrasound

2.1.2.1 Hydrogenation reactor

The base for all the kinetic studies carried out in this work was a semi-batch stirred tank reactor, as explained above. However, the system was modified in order to accommodate the ultrasound sources. Two different approaches were undertaken: an external oil bath provided with six transducers and an internal ultrasonic probe inserted directly into the reactor. Details about these two set-ups are given in the following two sub-sections.

a) External ultrasound source

This set-up provides indirect sonication to the reaction vessel, and the design is similar to an ultrasonic bath (Figure 1). The outer hull of the reactor was hexagonal with transducers mounted on the center of each face of the hull. Each transducer was able to deliver 100 W of power, 20 kHz of frequency, which was aimed toward the center of the bath. The stainless steel vessel was then put inside. The

bath was filled with silicone oil Rhodorsil® 47V 350 and warmed up to 170°C on a heating plate.

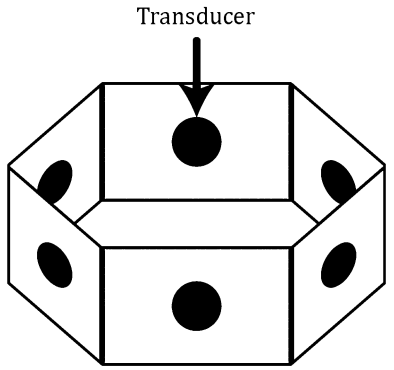

Figure 2.2. Hexagonal ultrasonic bath filled with silicon oil.

b) Internal ultrasonic source

Some modifications were done to the classical slurry reactor system in order to fit and implement an internal ultrasonic probe. The system is displayed in Figure 2.3.

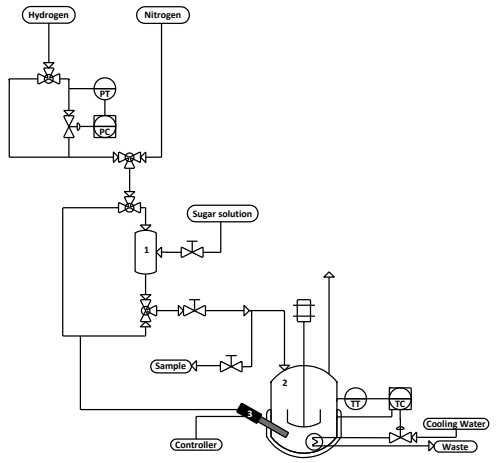

Figure 2.3. Scheme of the modified hydrogenation reactor system with an internal ultrasound source. The units: (1) reactor, (2) bubbling chamber, (3) internal probe.

The ultrasound source was obtained from Misonix, Inc., part no. S-4000 with a standard 0.5" horn (12.7cm x 3.8 cm) made in a titanium alloy. An automatic controller from Misonix, Inc. allowed the selection of the output power.

The purpose of installing an internal probe was to directly irradiate the medium and to know exactly how much power was delivered to the system. Due to the numerous components both inside (cooling coil, stirrer, sample line) and outside (engine and diverse lines) the reaction vessel, it was only possible to fit the probe by tilting it. However, this should not have any fundamental impact on the results, because of the small size of the vessel (ultrasonic waves are able to spread throughout the whole reaction volume) and the high stirring rates (1800 rpm) employed during the reaction, which guarantees a thorough contact of the reaction medium with the ultrasonic probe.

The probe was surrounded by a pipe that protected it and isolated it from any direct contact between the tip and the reactor walls; a pressurized hydrogen line was attached to the protecting pipe for equilibrating the pressure in the vessel.

2.1.2.2 Catalyst pre-treatment

a) Catalyst reduction procedure

For a selected number of experiments, the Ru/C catalyst was reduced before the reaction by placing it in the reactor. Once the setup was in place, oxygen was purged with a nitrogen flow for 10 minutes followed by hydrogen for additional 10 minutes. The temperature was set (two temperatures were tested: 110°C and 250°C) and, once the desired conditions were reached, the catalyst was left to reduce for two hours. Afterwards, the reactor vessel was cooled down to room temperature and the atmosphere was purged with nitrogen for 10 minutes. Finally, the sugar solution was fed as described in Section 2.1.2.3.

b) Catalyst pre-treatment with ultrasound

The same amount of catalyst as mentioned above was placed in a three-neck round-bottom glass flask (Figure 3). The flask was equipped with the ultrasonic probe, a thermocouple, a hydrogen line with a 7 μm filter to facilitate dispersion of the hydrogen in the solution, and a cooling column for the outlet gas. Then, 90 ml of deionized water were added (enough to cover the ultrasound probe). The reaction medium temperature was set to 25°C. Then the reactor was flushed with argon during 10 minutes, after which the sonication was activated for 10 min at 1 % of amplitude (10 W) under hydrogen flow. Finally, the glass flask was purged with argon and the medium was transferred into the hydrogenation reactor.

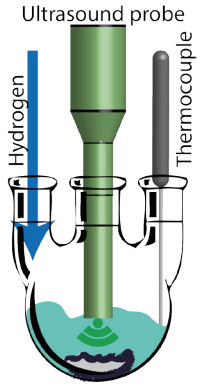

Figure 2.4. Catalyst pre-treatment setup.

2.1.2.3 Procedure

For galactose, a solution of 4 wt. % (Danisco, 98 % purity) was prepared. In the case of arabinose, solutions of 4 and 20 wt. % (Sigma Aldrich, 99 % purity) were prepared. In the cases when no pre-treatment was performed, 0.91 wt. % of Ru/C catalyst (relative to the mass of dry sugars) was directly placed into the reactor. Afterwards, a stream of nitrogen was passed through the vessel for 10 minutes; thereafter the sugar solution was fed into the bubbling chamber and, subsequently, flushed with nitrogen and hydrogen for 10 minutes. The vessel chamber was pre-heated at 90 °C.

Then the solution was fed into the reactor, and the nitrogen was purged with hydrogen according to the following two-step procedure: (i) increase the hydrogen pressure up to 10 bar and, (ii) release of the hydrogen down to a pressure just above atmospheric pressure (ca. 0.5 bar). This was repeated for a total of three times. Thereafter, the temperature and pressure were set to the reaction conditions. The experiments were carried out at 105°C and with pressures ranging from 30 to 50 bar. As soon as the conditions were reached, both the timer and the stirring were activated. No reaction was observed before starting the stirring. A stirring rate of 1800 rpm was maintained throughout the reaction to guarantee a kinetic regime.

The ultrasonic irradiation regimes varied from the external and internal sources. In the case of the external ultrasonic bath, a continuous setting of 100% was used. Instead, a pulsed regime was used for the internal probe to avoid promo-

tion of iron leaching. The pulse conditions were 10 seconds ON, and 5 minutes OFF for an overall time of three hours, with a mean power of 30 W.

a) Catalyst deactivation tests

To check for catalyst deactivation, three consecutive experiments were carried out. After each experiment, the product solution was withdrawn from the purge line, through the filter, thus leaving the catalyst inside the vessel. By doing so, the reactor was never opened and the catalyst remained in the inert nitrogen atmosphere. Between each experiment, the catalyst was washed three times with 100 ml of warm water.

2.1.3 Continuous hydrogenation

Catalytic hydrogenation reactions were carried out in a continuous three-phase system using three kinds of catalysts: carbon nanotubes supported on random stainless steel sponges (CSS), activated carbon clothes (ACC), and crushed commercial extrudates. The set-up consisted of a high pressure liquid metering pump (Eldex Optos 1SMP), an ohmic resistance for heating, and controllers for backpressure (Brooks 5866), gas mass flow (Brooks 5850S) and temperature (CAL Controls 9500P); the backpressure controller was located downstream whereas the mass flow controller was located at the inlet. The temperature was measured using two thermocouples: one placed inside the tube and the other on the outer core of the reactor (Figure 2.5).

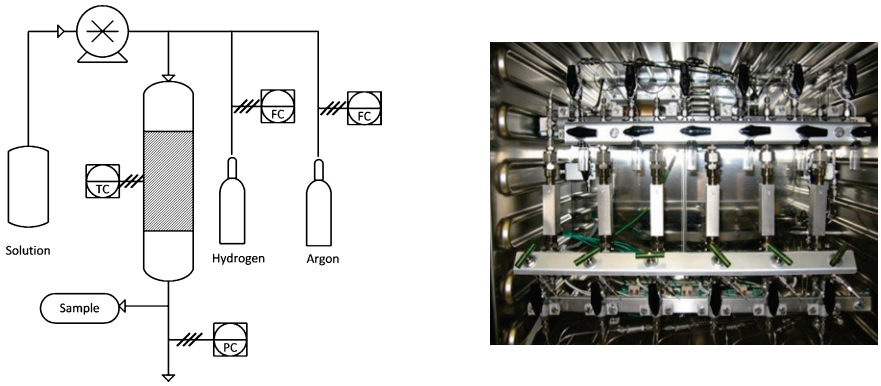

Figure 2.5. Continuous reactor set-up: process flow diagram (left) and photography (right).

The experiments were performed in a tube reactor having a length of 120 mm and an inner diameter of 12.5 mm. The operating conditions are described in

Table 2.1. For the structured catalysts (ACC and CSS) only one set of parameters were tested, whereas for the commercial ground extrudates a more thorough condition screening was carried out by the means of a 2_{IV}^{4-1} fractional factorial design.

Table 2.1. Operating conditions for the continuous hydrogenation

	ACC / CSS	Ground extrudates	
		Low	*High*
Temperature [°C]	130	120	140
H2/gas flow [ml/min]	50	100	200
Liquid flow [ml/min]	2	1	3
Catalyst particle size	-	[45:71]	[71:150]

Prior to every experiment, the reactor was purged during 15 minutes with argon to evacuate the oxygen from the system. The catalyst was reduced in-situ with H_2 flow (AGA 99.999%) at 200 °C for 150 minutes. After reducing the catalyst, the operating conditions of temperature and pressure were adjusted. The feedstock was bubbled with hydrogen for 10 minutes before each experiment to eliminate the oxygen from the solution and guarantee the hydrogen saturation. Subsequently, the solutions were fed through the piston pump. At this moment, the reaction was considered to have started and samples were withdrawn at intervals of 15 min during 2 to 2.5 hours of reaction.

2.2 Analytical methods and procedures

2.2.1 High-performance liquid chromatography (HPLC)

The off-line concentration analysis was conducted using a high-performance liquid chromatograph (HP 1100 Series LC) equipped with a Biorad Aminex HPX-87C carbohydrate column and coupled to a refractive index detector (HP 1047A).

The employed method consisted of a 2 μL sample injection and a mobile phase flow of 0.400 mL/min (aqueous solution of $CaSO_4$ 1.2mM) at 80 °C. The use of $CaSO_4$ as an inorganic modifier has been suggested to help regenerate the stationary phase calcium ions that might have been removed by interaction with ions derived from aldonic acids.[45] The elution order is presented in Table 2.2.

Table 2.2. Relative retention times of the studied sugars

Sugar	Retention time (relative to D-maltose)	Sugar	Retention time (relative to D-maltose)
D-Maltose	1.0	**L-Arabitol**	2.2
D-Galactose	1.4	**L-Rhamnitol**	2.4
L-Rhamnose	1.4	**D-Galactitol**	2.6
D-Maltitol	1.4	**D-Sorbitol**	2.7
L-Arabinose	1.6		

2.2.2 Acoustic power measurements

For measuring the ultrasonic power, the formation of tri-iodide ions from a KI solution was followed by UV spectrometry at 354 nm (Weissler reaction[46]). First, an I_2 solution (0.05M) was prepared by dissolving the corresponding amount of resublimed iodine in a potassium iodide solution. In an aqueous iodide solution, the insoluble iodine (I_2) molecules form soluble tri-iodide (I_3^-) ions, which were titrated against a 0.01M standardized solution of sodium thiosulfate. The solution was then diluted to obtain three different standards at 0.1 mM, 0.075 mM and 0.05 mM, and the spectrometer detector (Shimadzu 2550) was finally calibrated by measuring the absorbance of the prepared standards. After calibration of the spectrometer, 100 ml of a potassium iodide solution (25 % w/v) was poured into the standard reactor (see Section 2.2), the thermostat was set to 23 °C and the ultrasonic irradiation with the external source was carried out for 30 minutes at different output settings. The amount of produced tri-iodide was then quantified by the UV spectrometer. The results were compared with those obtained under the same conditions using the internal ultrasonic source (factory calibrated) in a glass reactor. The comparison provided an approximate evaluation of the acoustic power.

2.3 Catalyst characterization

2.3.1 Nitrogen adsorption

The surface area of the catalyst was determined by nitrogen physisorption (99.999%, AGA) using a Sorptomatic 1900 by Carlo Erba Instruments. First, the samples were outgassed under vacuum at 150 °C for three hours and the adsorption/desorption steps were carried at 77 K, using liquid nitrogen as coolant. The

adsorption data were interpreted with the Brunauer-Emmett-Teller (BET) isotherm.

2.3.2 Inductively coupled plasma optical emission spectrometry (ICP-OES) and Induced current plasma – mass spectrometry (ICP-MS)

A PerkinElmer SCIEX ICP Mass Spectrometer Elan 6100 DRC Plus and a Optima 5300DV ICP Optical Emission Spectrometer were used to measure the ruthenium contents in the catalyst and in the reaction medium.

2.3.3 Scanning electron microscopy (SEM)

Catalyst images as well as elemental analyses were obtained with a Leo Gemini 1530 scanning electron microscope equipped with a ThermoNORAN Vantage X-ray detector for EDXA analysis. The images were taken using the Secondary Electron and Backscattered Electron detectors at 15 kV, and the In-Lens Secondary Electron detector at 2.70 kV.

2.3.4 Transmission electron microscopy (TEM) and X-ray diffraction (XRD)

An energy filtered transmission electron microscope (EFTEM LEO 912 OMEGA, 120 kV) and a scanning electron microscope (SEM/EDS, Jeol JSM 6400) were used to study the microstructure of the support as well as the distribution, the size and the concentration of the catalyst metal. The crystal structure and the average size of catalyst were determined by using X-ray diffraction (Siemens D5000 with CuKα radiation).

2.3.5 Temperature programmed reduction (TPR) and CO pulse chemisorption

An AutoChem 2910 instrument (Micromeritics) was used for the measurements. The weighed sample was dried under helium at 400°C during 30 minutes, and then returned to room temperature. Subsequently, a mixture of H2/Ar 5 %/95 % was fed, while the system was heated up to 900°C following a temperature ramp of 10°C/min.

The same instrument was used for CO pulse chemisorption measurements. A weighed sample was reduced under hydrogen at 200°C during 150 minutes, and

then cooled down to 50 °C. Subsequently, pulses of a mixture of 10 % CO in He were introduced. A ratio of CO:Ru = 1:1 was assumed.[25]

2.4 Determination of physical properties

2.4.1 Density measurements

The density measurements for aqueous sugar solutions (L-arabinose, D-galactose, D-maltose, L-rhamnose) were carried out in an Anton-Paar DMA-512P oscillating U-tube density-meter equipment (±0.0001 g/cm^3), operating at a pressure range of 1-20 bar and between 60-130 °C. A Grant GP-200 (±0.1 °C) thermostatic bath with oil as a heating fluid was used to control the temperature within the measuring cell. In order to prevent inaccuracies in the system temperature due to heat loss, a thermocouple (±1 °C) was inserted directly into the measuring chamber to monitor its temperature. The system was pressurized with nitrogen (AGA 99.999 %) at 5 bar to prevent changes in the concentration of the solutions fed at high temperatures. The liquid density values were obtained directly from the device.

Solutions of 25 and 50 wt. % were prepared for each sugar sample. Before feeding each sample into the equipment, the measuring cell was cleaned several times with hot water and ethanol to wash out any impurity that could compromise the reliability of the measurement. The cell was flushed with nitrogen (AGA 99.999%) to dry it. The solution was fed in excess to evacuate gas bubbles using sterilized syringes. At this instant, all the valves were closed, the system was pressurized and it was considered to be the starting point of the measurement. Once the density values were recorded, the system was purged with water and ethanol several times.

2.4.2 Viscosity measurements

The viscosities of the different aqueous sugar solutions were measured using an Ostwald glass capillary viscometer, operating between 60-90 °C and at atmospheric pressure. Solutions of 25 and 50 wt. % were prepared for each of the studied sugars (L-arabinose, D-galactose, D-maltose, L-rhamnose).

The viscometer was filled with the different solutions and placed vertically in a Heidolph Ekt 3001 water thermostatic bath with a ±1 °C precision. Once the

thermal equilibrium was reached, the efflux times of the liquids were recorded with a digital stopwatch with a precision of ±0.01 s. The measurements were performed in quintuplets at the different conditions of temperature and composition to minimize errors.

The viscosity determination by using Ostwald viscometers is an indirect technique, i.e. the measured variable is not the viscosity itself but the efflux time of the liquid through the capillary in the viscometer. Once the efflux times are determined, the kinematic viscosity is obtained through Equation (2.1),

$$\nu_1 = \frac{t_1}{t_0} \cdot \nu_0 \tag{2.1}$$

where ν_0 [m^2/s] is the kinematic viscosity of a known fluid; t_0 [s] is the efflux time of the known liquid through the viscometer; t_1 [s] is the efflux time of the sample through the viscometer and ν_1 [m^2/s] is the kinematic viscosity of the sample. The dynamic viscosity (μ) of the sample is then obtained with the aid of the previously determined kinematic viscosity and the density of the solution.

The reference fluid was de-ionized water and its viscosity values were obtained from the literature.[47] The calibration of the viscometer with pure water was carried out for all the studied temperatures. To verify that the test solutions remained at their nominal concentrations within reasonable limits, solution samples were withdrawn before and after the determinations and analyzed by HPLC. No significant changes in concentration were observed.

2.4.3 Hydrogen solubility measurements

The hydrogen solubility of different aqueous solutions of the sugars were measured in-situ with a Fugatron HYD-100 equipped with a polymeric perfluoroalkoxy co-polymer (FPA) hydrogen-permeating probe, operating between 90-130 °C and 10-60 bar. Table 2.3 shows the different sugar solutions used for the hydrogen solubility measurements. The Fugatron probe was attached to the batch reactor described in Section 2.1.1.

After feeding the different sugar solutions into the system, the reactor was purged with nitrogen for 15 min to evacuate oxygen. The gas inlet was switched to hydrogen and the Fugatron was switched on. Subsequently, pressurization

with hydrogen and heating took place simultaneously until the desired operating conditions were reached. Stirring was set to 1000 rpm to achieve a fast mass transfer to the surface of the probe.[48] At the given temperature, pressure and stirring conditions, the system was left to stabilize during 15 min to guarantee that the solution was saturated with hydrogen and then the values of hydrogen concentration were recorded.

Table 2.3. Sugar solutions for hydrogen solubility measurements.

Sample	Concentration [wt. %]
L-arabinose	10
L-rhamnose	10
D-maltose	10
D-galactose	4

2.4.3.1 Calibration of the Fugatron HYD-100

The Fugatron HYD-100 gives only information about the concentration (in ppm) of the permeated hydrogen from the solution into the carrier gas. Hence, a calibration of the equipment needs to be done before any measurement to estimate the equipment calibration constant (f), which correlates to the concentration of hydrogen in the liquid bulk via the following Equation (2.2),

$$C_{L,H_2} = f \cdot C_{Gc,H_2} \tag{2.2}$$

where C_{L,H_2} [mol/L] is the concentration of hydrogen in the bulk; and C_{Gc,H_2} [ppm H_2] is the concentration of hydrogen permeated in the carrier gas.

The calculation of the calibration constant was done as follows. The system was loaded, heated and pressurized, following the procedure described in Section 2.4.3. The amount of the sample fed (V_L) and the first state of pressurization (P_0) were arbitrary, although these values were registered. The temperature of the calibration was the same as in the measurements, since the calibration is highly temperature dependent.

Subsequently, the Fugatron equipment and stirring (1000 rpm) were turned on. The system was let to stabilize. Once the reading at Fugatron was constant, the stirring was stopped, an step disturbance in hydrogen pressure (P_1) was intro-

duce into the system. Stirring was turned on (1000 rpm) and the system was let to stabilize to guarantee saturation of the sample with hydrogen. After 15 min, the hydrogen absorption would reach equilibrium at pressure P_2. At this moment P_2 and the value reported by the Fugatron (C^*_{Gc,H_2}), were registered.

The registered values of V_L, P_0, P_1 and P_2, were used in Equation (2.3) to calculate the Henry's constant of the sample [48],

$$\frac{1}{He} = \frac{(P_1 - P_2)}{(P_2 - P_0)} \cdot \frac{V_G}{V_L} \cdot \frac{1}{R \cdot T} \tag{2.3}$$

where He is Henry's constant [L·atm/mol]; P_1 is the initial pressure before absorption; P_2 is the equilibrium pressure after absorption; P_0 is the equilibrium pressure of the lower initial pressurization state; V_G is the volume of the gas phase; V_L is the volume of the liquid phase; R is the universal gas constant [0.082 L·atm/mol·K]; and T is the temperature of the system [K].

Once the Henry's constant was obtained, the saturation concentration of hydrogen in the bulk was calculated from Equation (2.4). Finally, the calibration constant was calculated through Equation (2.5),

$$C^*_{L,H_2} \cdot He = \mathrm{P}_2 \tag{2.4}$$

$$f = \frac{C^*_{L,H_2}}{C^*_{Gc,H_2}} \tag{2.5}$$

where f is the calibration constant, C^*_{L,H_2} is the saturation concentration, and C^*_{Gc,H_2} is the equilibrium concentration in the Fugatron after absorption (P_2).

2.5 Catalyst preparation

A summary of the preparation of the catalysts employed throughout the study of the continuous set-up is presented in Table 2.3. Details about the preparation of the catalysts are given in the following sub-sections. The active metal present in all catalysts was ruthenium.

Table 2.4. Tested catalysts

Support	Batch	Support pretreatment	Impregnation solvent	Method	Ultra Sound
Active carbon clothes (ACC)	1	No	Ethanol	Impregnation	No
	2	No	Acetone		No
	3	Yes	Acetone		Yes
	4	Yes	Acetone		No
Carbon wash-coated steel structures (CSS)	1	No	Water		No
	2	No	Water	Incipient wetness	No
Active carbon	Crushed commercial catalyst Particle size distributions: [45:71 μm] and [71:150 μm]				

2.5.1 Preparation of Ru/Active carbon cloth (Ru/ACC) catalyst

Before beginning the impregnation process, a batch of the clothes (Figure 2.6) was pre-activated in solutions of HNO_3 and H_2O_2 while the remaining batch was not pre-activated at all.

Figure 2.6. ACC support

The pre-activation consisted of a treatment with 5 wt.% HNO_3 aqueous solution at 80 °C for three hours to introduce oxidic surface group. Afterwards, the cloth was carefully washed and placed in a solution containing 2 ml of H_2O_2 30 w% in 100ml of DI-water at 60 °C for 2 hours. Finally, the support was removed from the bath and left to cool down in the solution for 2 more hours.

After pre-activation, the clothes were washed first in ethanol and then left to dry overnight at 60 °C. Afterwards, a solution of $RuCl_3$ in either ethanol or acetone was prepared (the amount of $RuCl_3$ was calculated aiming at a 5 wt.% of Ru loading on the support) and the clothes were submerged in this solution and made rotate by means of a mechanical stirrer. The beaker containing the solution and the support was submerged in a cooling bath (-10 °C) for 20 hours to prevent the ethanol solution from evaporating and promote the exothermic adsorption process. Once passed the impregnation time, the clothes were removed from the solution and washed with abundant deionized water. For guaranteeing a complete removal of the chlorine ions, the clothes were submerged in a basic (pH=13.20) NaOH solution under mild stirring for 24 hours. The clothes were washed with water and dried under vacuum at room temperature. Ultrasound irradiation during impregnation was tested, too.

2.5.2 Preparation of Ru on carbon wash-coated steel (Ru/CSS) structures

No pretreatment was carried out on these structures (Figure 2.7). The deposition of ruthenium was achieved by either one of two methodologies: the first one resembles that of the Ru/ACC, only that water was used as a solvent, thus eliminating the need to chill the precursor solution. The second technique was based on the incipient wetness method as explained in the following.

Figure 2.7. CSS support

A concentrated $RuCl_3$ solution, containing the incipient wetness amount of solvent (maximum liquid volume that can be taken up by the support without overflowing), and a calculated amount of Ruthenium (5wt. % of the support) was prepared. The solution was added to the support and it was left to dry overnight at room temperature and then in the oven for 3 hours at 80 °C. To guarantee a complete removal of water, the sample was further heated in a quartz oven under a N_2 flow at 120 °C for 1 hour. Subsequently, the catalyst was reduced in a flow of 10% H_2/N_2 for 2 hours at 400 °C. Finally, passivation was carried out by applying

a gas flow with a concentration profile of 1%/5 min of O_2. Nitrogen was used as a carrier gas.

3 Results & Discussion

3.1 Anomeric equilibria of sugars

The analyzed sugars were predominantly in their pyranose form, as this is, generally speaking, the most stable form. However, a shift towards the more strained furanose form was observed in all sugars (except for L-rhamnose) at 90 °C. Refer to Figure 1.2 for the representation. D-maltose does not exhibit a furanose form as the hydroxyl group on the C-4 of the reducing end is "protected" by the glucosyl moiety.

Table 3.1. Mutarotational equilibrium of sugars at different temperature of the different forms of each of the four sugars.*

	Pyranose						Furanose					
Sugar	α			β			α			β		
	25°C	50°C	90°C	25°C	50°C	90°C	25°C	50°C	90°C	25°C	50°C	90°C
L-ara	62.5%	54.6%	45.8%	31.2%	33.8%	29.8%	4.2%	6.8%	13.4%	2.1%	4.6%	11.0%
D-gal	3.2%	5.1%	12.1%	63.6	62.0%	50.7%	1.9%	3.0%	8.1%	31.3%	30.0%	29.2%
D-mal	41.2%	39.7%	44.3%	58.8%	60.3%	55.7%	N/A					
L-rha	64.9%	62.1%	60.0%	35.1%	38.0%	40.1%	<2%					

**) The NMR experiments were carried out by Prof. Rainer Sjöholm and Ms. Päivi Pennanen at the Laboratory of Organic Chemistry, Åbo Akademi.*

3.2 Characterization results of fresh catalyst

A fresh commercial Ru/activated carbon catalyst was employed for the kinetic experiments and it consisted of a powder made up of small flakes with a cross section of 10×10 μm and an average thickness of 1-2 μm. BET analysis gave a total surface area of 690 m^2/g. The active metal content was determined to be 2.5 wt. % by ICP-OES. The TEM studies revealed that ruthenium was present as particles with diameters ranging from 2 to 3 nm.

After conducting each experiment, the contents of the reactor were stored and a number of samples were withdrawn and filtered, and the solution was analyzed

using ICP-OES to discover traces of leached ruthenium. The analysis showed that the metal content in the solution was below the detection limit of the instrument (0.9 mg/L), which confirms that leaching, if any, was negligible.

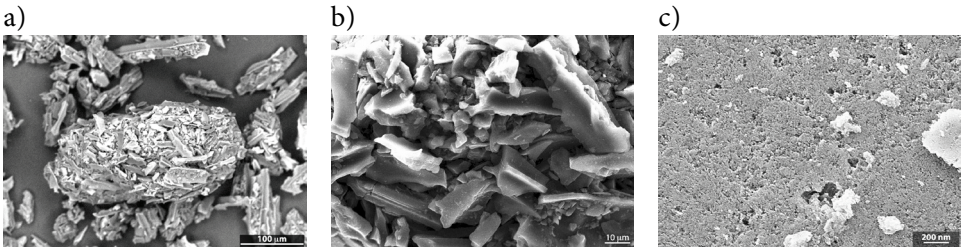

Figure 3.1. SEM images of the Ru/C catalyst at different magnifications: a) 250X, b) 1000X and c) 50000X.

The characterization results are summarized in Table 3.2. Some SEM and TEM images of the catalyst are provided in Figures 3.1 and 3.2.

Table 3.2. Catalyst characterization results

Property	Value
Catalyst	Ruthenium over active carbon
Surface Area	690 m^2/g
Ruthenium content	2.5 %(w/w)
Ruthenium particle size, determined by TEM (Figure 3.2)	2 – 3 nm (mono-dispersed particles)
Ruthenium leaching	< 0.9 mg/L
Particle Shape	Flakes
Particle average size	10 µm × 10 µm
Particle average thickness	1-2 µm

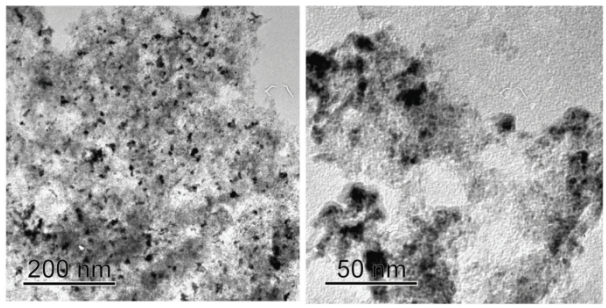

Figure 3.2. TEM images of the Ru/C catalyst.

3.3 Characterization of structured catalysts

The characterization of the studied catalysts is summarized in Table 3.3. Out of the two investigated support materials, the most promising of structured catalysts were the active carbon clothes (ACC). This material is by far superior in regards of surface area to the more common active carbon powders employed in previous studies.[49] Despite the low metal content, the ACC-based catalysts exhibit an efficient deposition of the active metal (small metal clusters and relatively high dispersion), which is comparable with tested commercial catalysts. Ultrasound had a detrimental effect in the metal cluster size and its distribution on the surface of the support. The same can be said about the effect of support pretreatment, though in this later case the effect is much less marked.

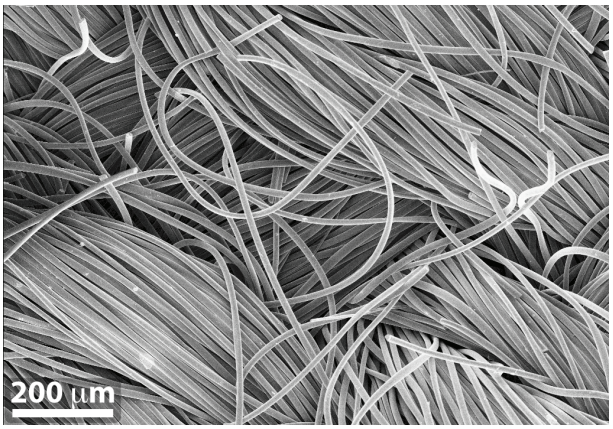

Figure 3.3. SEM image of ACC support

The best conditions for impregnating active carbon clothes seem to be those were no pre-treatment and no ultrasonic irradiation are involved and only the precursor solution and the support are left to interact. When it comes to the precursor solution, $RuCl_3$ dissolves readily in ethanol and acetone and with much more difficulty in water. Of the previously named two organic solvents, it surfaces that the ethanolic solutions produced catalyst with a richer metal content albeit a lower dispersion and bigger metal clusters.

The impregnation technique proved to be inappropriate for the deposition of ruthenium on the carbon nanotubes grown on the metallic structures. Although the amount of ruthenium that adhered to the support surface was comparable to that of the carbon clothes, the dispersion and ruthenium cluster size were evi-

dently worse. Moreover, and due to the nanoporosity of the carbon nanotube coating, it was not possible to determine the surface area of the support with the available techniques.

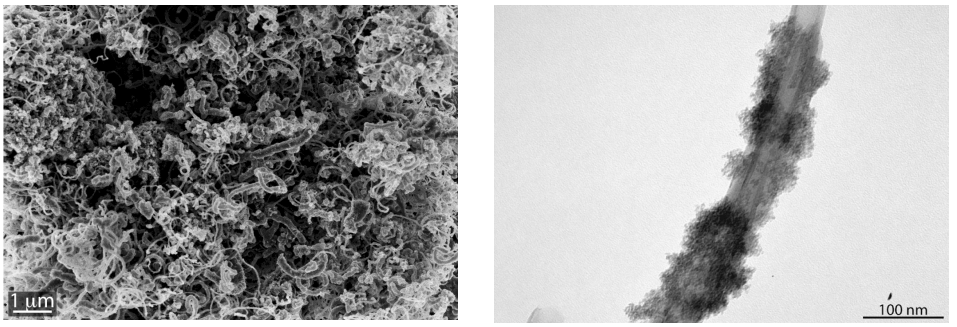

Figure 3.4. Ru/CSS catalyst (CSS#1): SEM (left) and TEM (right).

Table 3.3. Characterization of the tested catalysts

Catalyst	Ruthenium content [wt. %]	Surface area [m^2/g]	Dispersion	Metal cluster size [nm]
ACC#1	0.30 %	2000	8.32%	16
ACC#2	0.08%		21.80%	6
ACC#3	0.11%		8.40%	16
ACC#4	0.10%		17.42%	8
CSS#1	0.18%	Not detected	2.37%	56
CSS#2	0.05%		1.66%	80
Extrudates [45:71 µm]	0.70%	-	25.68%	5
Extrudates [71:150 µm]	0.70%	-	18.80%	7

3.4 Sugar physical properties and correlations

The discussion in this section will be approached in a generic manner since the four studied sugars (L-arabinose, D-galactose, L-rhamnose and D-maltose) exhibit the same behavior in each of the studied physical properties (density, viscosity and hydrogen solubility).

3.4.1 Density

The dependence of the density on the temperature of the system can be described as inversely lineal, i.e. the higher the temperature, the lower the density. The opposite can be said regarding the dependence on the concentration and a linear tendency of the density to augment with an increase of the sugar concentration was observed. This behavior is rather typical.

The density values were correlated by multivariable non-linear regression, which resulted in an empirical polynomial expression that represents the behavior of density as a function of temperature and concentration (Equation (3.1)).

$$\rho\left[\frac{kg}{m^3}\right] = -A \cdot T \cdot C_S + B \cdot C_S^2 + C \cdot C_S + D - E \cdot T + F \cdot T^2 \qquad (3.1)$$

where A, B, C, D, E and F are regressed constants, T [°C] is temperature of the system and C_S (wt. %) is the concentration of the solution. The parameters are summarized in Table 3.4.

Table 3.4. Parameters for density estimation (Equation (3.1)) [kg/m³]

	Parameters					
Sugar	***A***	***B***	***C***	***D***	***E***	***F***
L-ara	0.008154	0.008424	4.797	1065	1.627	0.005412
D-gal	0.007364	0.012000	4.684	1052	1.345	0.003999
L-rha	0.007629	0.000561	4.225	1040	1.071	0.002542
D-mal	0.005516	0.007905	4.573	1066	1.640	0.005373

Figure 3.5 shows how the behavior of the density of L-arabinose changes with temperature and concentration. It is also possible to observe that there are no unexpected irregularities that could arise due to the empirical and polynomial nature of the model. Nevertheless, extrapolations outside the given ranges should be done carefully given that the applicability of the correlation has yet to be validated.

3.4.2 Viscosity

An exponential decline of the viscosity with increasing temperature was observed. Concentration had a great impact on viscosity.

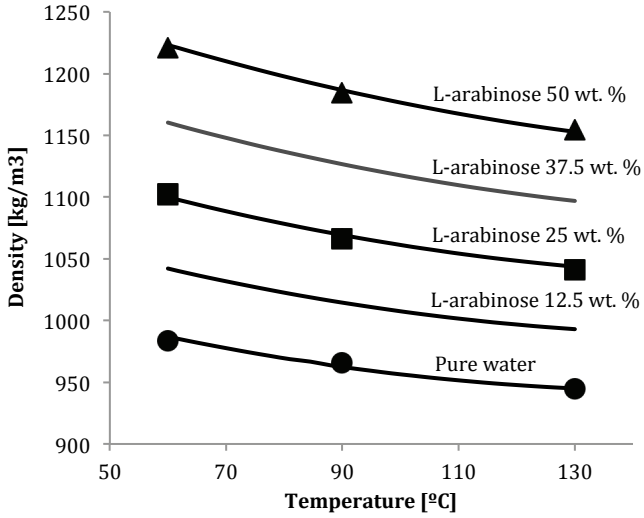

Figure 3.5. Density of L-arabinose. Experimental values (markers) and calculated values (lines).

Viscosity can be correlated as a function of temperature and concentration by the following expression proposed in the literature [50]:

$$ln(\mu) = \left(\frac{a + b.C_S}{1 + c.C_S}\right) + (\alpha + \beta.C_S^2).\left(\frac{1}{T} - \frac{1}{T_0}\right) \quad (3.2)$$

where a, b, c, α and β are constants, C_{Sugar} is the concentration of the solution in molal units [mol/kg H_2O], T [K] is the temperature of the system and T_0 is an assumed reference temperature (298 K). The parameters are listed in Table 3.5.

Table 3.5. Parameters for viscosity estimation (Equation (3.2)) [mPa·s]

	Parameters				
Sugar	a	b	c	α	β
L-ara	0.161	0.24	- 0.045	2297	35.87
L-rha	0.055	0.279	- 0.033	2075	36.852
D-gal	0.178	0.256	- 0.047	2331	34.755
D-mal	0.122	0.275	- 0.047	2216	36.852

A numerical regression was performed and the best parameters were estimated by minimizing the value of the square sum of errors (SSE). Acceptable agreement was found between measured and calculated values. Figure 3.6a shows how Equation (3.2) represents the tendencies of viscosity with respect to temperature and concentration.

An empirical expression is also proposed for representing the values of viscosity as a function of temperature and concentration (Figure 3.6b). The fit was performed by multivariable non-linear regression, which resulted in a multivariable non-linear polynomial expression (Equation (3.3)).

$$ln(\mu) = A.\frac{C_S}{T} + B.{C_S}^2 + C.C_S + D + \frac{E}{T} + \frac{F}{T^2} \quad (3.3)$$

where A, B, C, D, E and F are empirical constants, T is temperature in °C and C_S is the value of concentration in wt. %. The parameters are listed in Table 3.6.

Table 3.6. Parameters for viscosity estimation (Equation (3.3)) [mPa·s]

	Parameters					
Sugar	***A***	***B***	***C***	***D***	***E***	***F***
L-ara	1.544	0.0003808	-0.011000	-2.845	193.763	-3892
D-gal	1.540	0.0004631	-0.012000	-2.805	186.763	-3601
L-rha	1.466	0.0003216	-0.006641	-1.798	45.881	1185
D-mal	1.528	0.0004951	-0.011000	-2.628	164.305	-2925

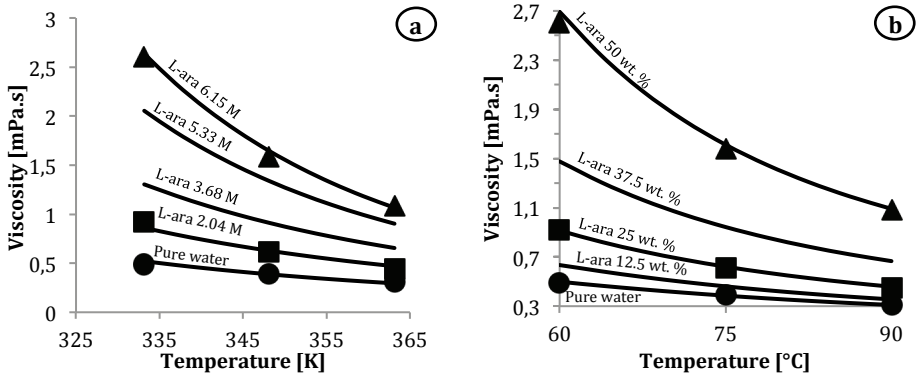

Figure 3.6. Viscosity of L-arabinose. Experimental values (markers) and calculated values (lines): (a) Migliori equation, (b) empirical expression.

As with the polynomial expression for the prediction of the sugar density, care should be taken when extrapolating outside the ranges of temperature and concentration since its applicability outside such intervals is not guaranteed.

3.4.3 Hydrogen solubility

Hydrogen solubility in aqueous solutions of sugars showed to have a tendency to increase exponentially with respect to the temperature of the system, whereas a linear dependence of the hydrogen solubility with the pressure was observed.

An empirical expression is proposed to represent the values of hydrogen solubility as a function of temperature and pressure.

$$C_{H_2} = A \cdot P_{H2} \cdot T + B \cdot T^2 + C \cdot T + D + E \cdot P_{H2} + F \cdot P_{H2}^2 \qquad (3.4)$$

where *A, B, C, D, E* and *F* are empirical constants; T [K] is the temperature of the system; P [bar] is the pressure of the system; and C_{H_2} [mol/L] is the hydrogen concentration in the liquid bulk.

Table 3.7. Parameters for hydrogen solubility (Equation (3.4)) [mol/L]

Sugar	Parameters					
	A [$\times 10^{-6}$]	B [$\times 10^{-4}$]	C [$\times 10^{-3}$]	D	E [$\times 10^{-3}$]	F [$\times 10^{-8}$]
L-arabinose 10 wt. %	9.35	0.01447	-1.138	0.222	-2.833	-0.1481
D-galactose 4 wt. %	8.888	-1.286	0.9355	-0.171	-2.456	0.07407
L-rhamnose 10 wt. %	6.921	0.0123	-0.9278	0.173	-1.865	-0.1481
D-maltose 10 wt. %	8.422	0.03372	-2.593	0.497	-2.504	-7.63

The fit was again carried out by built-in multivariable non-linear regression, resulting in an empirical polynomial expression, which represents hydrogen solubility as a function of temperature and concentration (Figure 3.7). Good agreement between the generated and experimental values of hydrogen solubility was obtained by using the proposed empirical correlation (Equation (3.4)).

Nonetheless, analogous treatment of this proposed correlation in terms of applicability outside the given ranges has to be given as in the cases of density and viscosity.

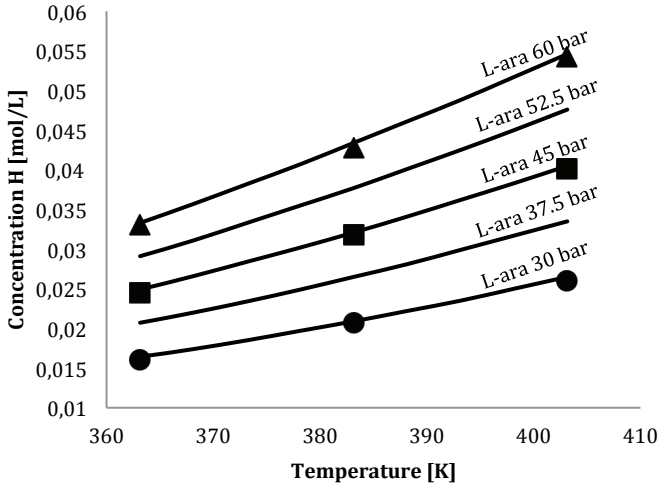

Figure 3.7. Hydrogen solubility in 10 wt. % L-arabinose solutions. Experimental values (markers) and calculated values (lines).

3.5 Qualitative kinetics

The hydrogenation behavior of the four selected sugars was similar in terms of the pressure and temperature influence. The effect of the hydrogen pressure was minor, whereas the temperature effect was very profound.

As will be described more in detail in the next section, the sugar hydrogenation was well-described by a Langmuir-Hinshelwood mechanism and exhibits a concentration-dependent reaction order, which ranges from zero order at high concentrations to first-order at low concentrations. However, the hydrogen pressure dependence was slight, which could explain the absence of a maximum in the reaction rate (as would be expected for a reaction proceeding via this kind of mechanism).

3.5.1 Pressure effect

The pressure effect was rather weak for the four studied sugars. D-galactose was an extreme case in that it exhibited an almost invariant behavior, i.e. close to zero order with respect to hydrogen. This is in agreement with the hydrogenation behavior of xylose over a range of different catalysts in which the kinetics become independent of the operating pressure at values exceeding 40 bar.[44]

3.5.2 Temperature effect

It was possible to draw conclusions about the influence of the temperature on the hydrogenation kinetics (Figure 3.8). As can be observed, the reaction temperature has a much more significant effect on the hydrogenation with the rates becoming considerably faster as the temperature increases. This remains true for all the four sugars. The apparent activation energies were in the range of 56 - 84 kJ/mol. The orders of magnitude of these activation energies are in accordance with values reported in the literature for the hydrogenation of D-glucose.[11,31,33,51]

3.5.3 Products and by-products

Typically, the selectivity towards the sugar alcohol is high both on sponge Ni and Ru catalysts, exceeding 95% under optimal conditions. Such data have been reported for the hydrogenation of glucose, xylose and lactose.[24,28,33–35] For some special cases, such as hydrogenation of fructose to maltitol, the product selectivity is a serious issue, the highest selectivities limited to about 60 - 70% on Cu-based catalysts.[36]

It was possible to reach complete conversion of the sugar molecules to yield the desired sugar alcohols as predominant products. This qualitative observation is primarily based on the direct inspection of the chromatograms. The by-product formation was very much dependent on the sugar in question: for L-arabinose and D-galactose, a relatively negligible by-product yield was observed, whereas in the case of D-maltose and L-rhamnose, the by-product formation was more important, though still significantly smaller than the main desired product. In the case of D-maltose, the most relevant by-product, which was readily identified during the HPLC analysis, was D-sorbitol (assumed to be yielded directly from D-maltitol as shown in Figure 1.3).

The by-product yields were observed to be dependent on the operating conditions: the more severe the conditions (higher pressures and temperatures), the more diverse and abundant the by-products, amounting to ca. 10-12 % of the total product yield under the more severe conditions for D-maltose and L-rhamnose, and to ca. 5-7 % for L-arabinose and D-galactose under the same severe conditions. However, in the majority of conditions, the by-product yields were less than 1%.

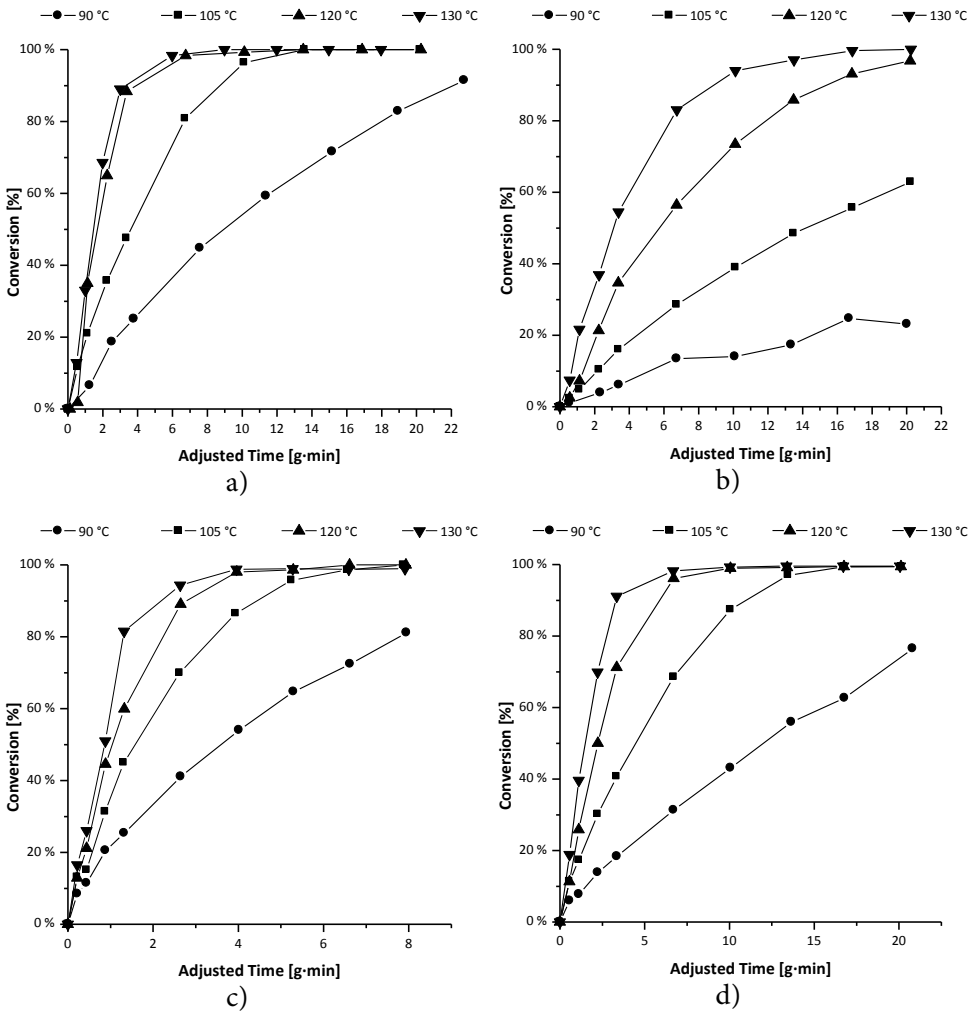

Figure 3.8. Temperature effect on the hydrogenation rates at 60 bar for L-arabinose and b) D-maltose, c) D-galactose and d) L-rhamnose.

3.6 Hydrogenation of sugar mixtures

3.6.1 Effect of sugar molar ratios

To study the influence of the sugar molar ratios on the hydrogenation kinetics of both sugars (L-arabinose and D-galactose) in the mixture, several experiments were carried out at different molar ratios of D-galactose to L-arabinose (0.1-10), being the average ratio of galactose-to-arabinose units in arabinogalactan (a hemicellulose) about 5:1.[52]

Typically, very high yields (close to 100%) and selectivities (95-99%) were achieved, the products being arabitol and galactitol. No by-products were detected.

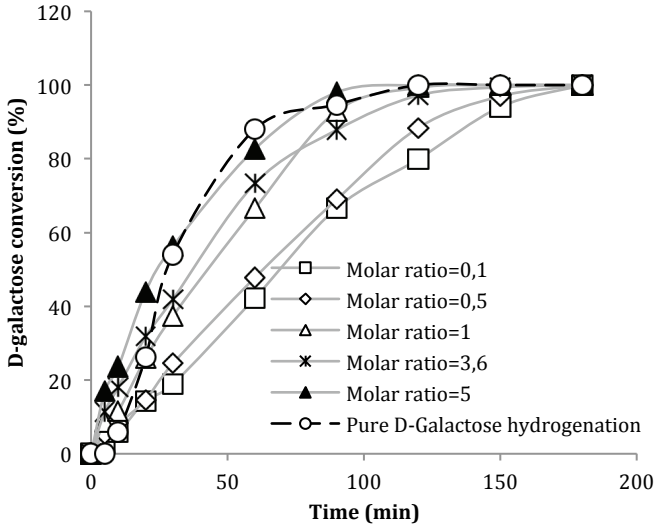

Figure 3.9. Effect of the molar ratio on the hydrogenation of D-galactose in the presence of L-arabinose at 120°C and 40 bar.

In the case of D-galactose (Figure 3.9), the hydrogenation in the mixture did not exhibit any unexpected behavior: the higher the concentration of galactose in the mixture was, the faster the reaction proceeded with no important difference between the limiting case of pure sugar and the higher ratios. The behavior displayed in Figure 3.9 can be explained by a competitive adsorption effect: the presence of a competing sugar retards the hydrogenation rate of the other sugar.

However, L-arabinose exhibited an acceleration of the rate with an increased amount of D-galactose (Figure 3.10), starting from 0.1 and stabilizing at ratio 1 (ratios 2 and 3.6 presented a small variation). The most remarkable observation is that at ratio 5 (i.e., the concentration of D-galactose being 5 times that of L-arabinose) the reaction proceeded even faster than the limiting case of pure arabinose. This effect was very clear as confirmed by Figure 3.10. As contradictive as this observation appears to be at first glance, rate accelerations in the presence of parallel reactions competing for a common reagent (in this case hydrogen) had been observed and studied before, both theoretically and experimentally.[53]

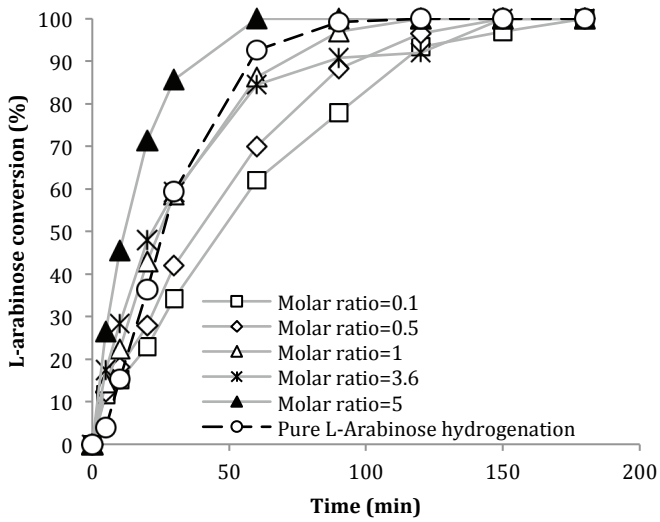

Figure 3.10. Effect of the molar ratio on the hydrogenation of L-arabinose in the presence of L-arabinose at 120°C and 40 bar.

3.6.2 Temperature effect

In the experimental temperature range (90-120 °C), the reaction rates of arabinose and galactose were found to increase with increasing temperature (Figure 3.11 and Figure 3.12). This behavior is to be expected and has also been observed in the hydrogenation of other sugars (glucose, fructose, lactose and xylose).[24,25,28,31,35,51] The apparent activation energies for L-arabinose and D-galactose were found to be 50 kJ/mol and 60 kJ/mol, respectively. Temperatures exceeding 120 °C were not studied due to increased by-product formation and sugar degradation.[49]

3.6.3 Hydrogen pressure effect

Several experiments were performed to study the effect of hydrogen pressure on the hydrogenation kinetics of mixtures under operating conditions of 40, 50 and 60 bar and 105 °C, and at two different molar ratios. It was found from these experiments that the influence of the hydrogen pressure on the reaction rate was insignificant, i.e. the kinetics was close to zero order with respect to the hydrogen pressure. This is in accordance with the hydrogenation of pure sugars, where the influence of hydrogen pressure is only slightly stronger.[49]

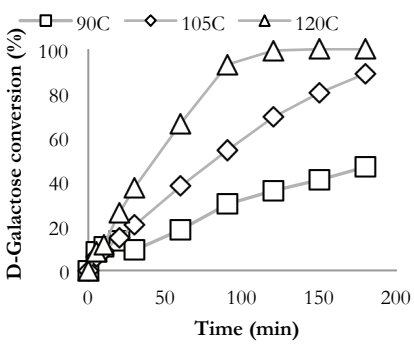

Figure 3.11. L-arabinose and D-galactose hydrogenation. Molar ratio 1, 40 bar.

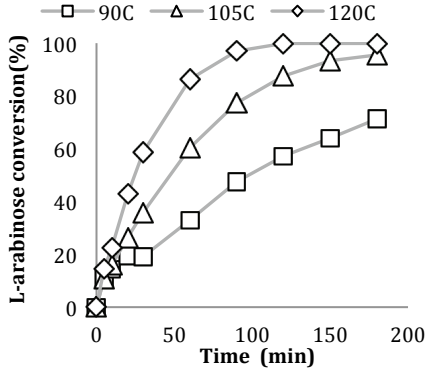

Figure 3.12. L-arabinose and D-galactose hydrogenation. Molar ratio 1, 40 bar.

3.6.4 Product yield and selectivity

An overall selectivity towards both sugar alcohols was typically 99% in the performed experiments. As discussed in the previous section, an influence of the temperature on by-product formation was observed. The maximum by-product formation was about 5% under the more severe conditions of temperature and pressure (120 °C and 60 bar); otherwise, it was close to 1%.

3.7 Ultrasound-assisted hydrogenation

3.7.1 Sugar hydrogenation under silent and sonicated conditions

Previous studies on xylose and lactose hydrogenation have demonstrated that ultrasound treatment could improve the catalyst performance by retarding the catalyst deactivation. The experiments reported in the literature were performed in the presence of sponge nickel. In order to reveal, whether similar effects are also possible for ruthenium catalysts, a series of experiments was carried out. L-arabinose and D-galactose were used as model molecules.

3.7.1.1 Influence of the sugar nature

a) Arabinose hydrogenation

The results of three consecutive experiments under silent and sonicated conditions are displayed below (Figure 3.13).

Despite the kinetics of the first experiment being the same under both silent and sonicated conditions, the deactivation seems to be stronger for the successive experiments. Indeed, the second and third experiments showed slower hydrogenation kinetics under ultrasound than the third experiment under silent conditions. The catalyst deactivation seems to be slightly worsened.

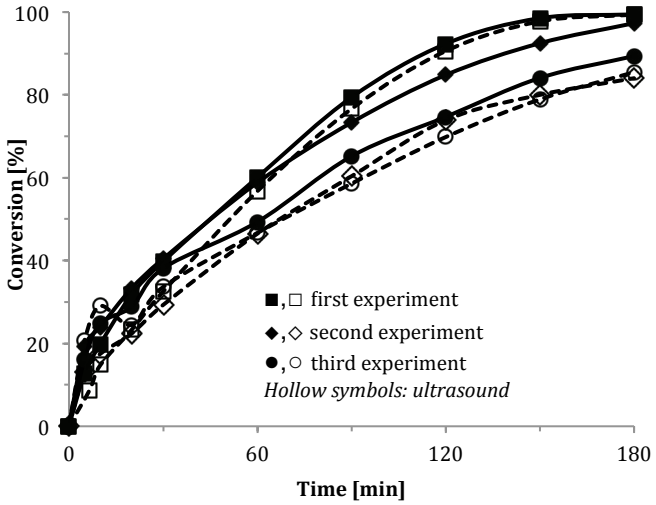

Figure 3.13. Impact of ultrasound (external source) on the catalyst deactivation with arabinose (105 °C and 50 bar).

b) Galactose hydrogenation

A catalyst deactivation study under silent and ultrasound conditions with galactose is presented in Figure 3.14.

Only the first experiment with galactose under acoustic irradiation showed a significant enhancement of the hydrogenation rate. This positive result was not observed on the kinetics of the second and third experiments: they were very much the same as under silent conditions. Therefore, no rejuvenation of the Ru catalyst was achieved by ultrasound implementation.

3.7.1.2 Influence of pressure

No positive effects for the process intensification were observed under the original conditions (105 °C, 50 bar). A hypothesis to explain the results was that the power delivered to the system was too low to clean the catalyst surface and to disperse it.

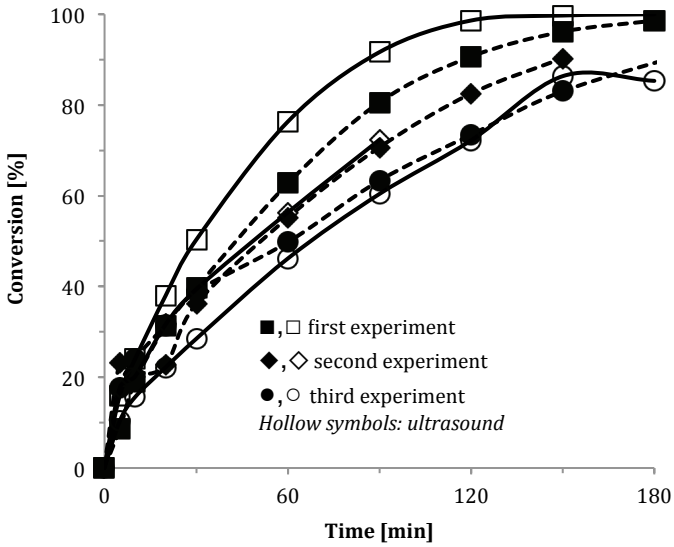

Figure 3.14. Impact of ultrasound (external source) on the catalyst deactivation with galactose (105 °C and 50 bar).

At really high pressures, the medium pressure could be higher than the amplitude pressure of the ultrasound and then, it is assumed that there will not be any negative pressure resultant, hence no cavitation.[54,55] In order to test this hypothesis, experiments at lower pressures were performed. Since previous studies have shown that mass transfer limitations of hydrogen prevail below 30 bar, the pressure range was set to 30-50 bar. The impact of the hydrogen pressure under silent and sonicated conditions was studied and the results were described in the following graphic (Figure 3.15).

The kinetics under silent conditions was not influenced by external pressure in this range. However, under sonicated conditions, the effect of ultrasound decreases with the pressure, in contradiction to our hypothesis. This points at the notion that the benefits of ultrasound disappear with more intensive ultrasonic exposure, either by a long-term treatment (reuse) or by higher effective irradiation achieved at lower pressures.

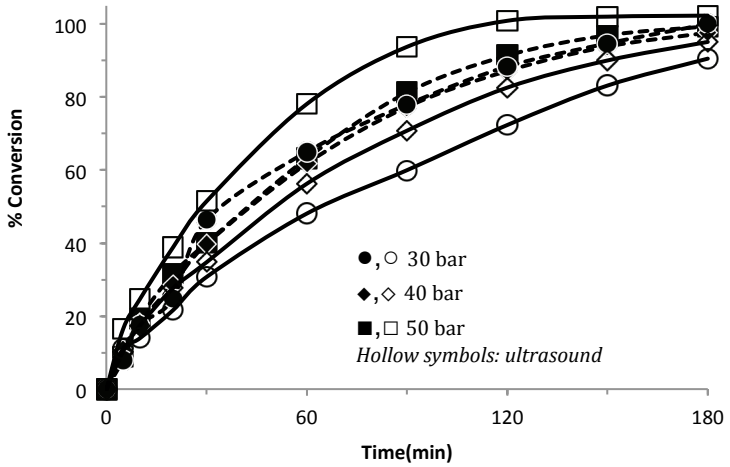

Figure 3.15. Impact of the pressure on the hydrogenation kinetics of galactose at 105°C.

3.7.1.3 Influence of concentration

The effect of the concentration of the sugar solution on the ultrasonic performance was also studied to seek explanations to the observed differences between arabinose and galactose, which were hydrogenated at different concentrations. The effect of the arabinose concentration on the system both under silent and acoustic conditions was explored by using a solution at 4 wt. % of sugar and comparing with the results previously obtained by using sugar solutions of 20 wt.% concentration.

The experiments performed at lower concentration of arabinose under ultrasound gave very similar kinetics compared to silent conditions, that is no enhancement by ultrasonic irradiation, which in turn confirms the trend observed at higher concentrations. Thus, the differences observed between galactose and arabinose cannot be attributed to the concentration difference of the starting solutions.

3.7.2 Internal ultrasound source (probe)

The results obtained with an internal ultrasound probe are presented in Figure 3.16. No favorable impact of the ultrasound on the hydrogenation rate was observed. The reaction rates were even slower in the presence of ultrasound.

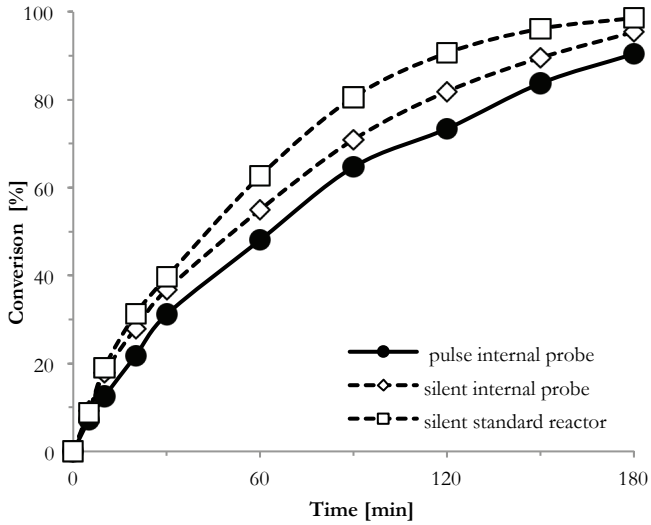

Figure 3.16. Comparison of pulsed ultrasound with silent conditions in the standard reactor: hydrogenation of D-galactose 4%, 105 °C, 50 bar.

Unfortunately, it was not possible to screen other power outputs to confirm this result due to technical limitations of the apparatus. A power output of 30 W was the lowest limit that could be reached under the operating pressure (50 bar), while higher power outputs produced unsteady oscillations (sudden power drops to ~30W) and might promote iron leaching from the reactor walls.

3.7.2.1 Pre-treatment

In order to prevent any poisoning by iron leaching from the reactor walls under ultrasound, and to have a direct irradiation of the catalyst, the catalyst pre-treatment with ultrasound was studied. The results are displayed in Figure 3.17.

No enhancement of the kinetics due to the pre-treatment was observed, implying that there is no impact even with a guaranteed cavitation regime (atmospheric conditions) and absence of iron leaching.

3.8 Modeling results

3.8.1 Hydrogenation of individual molecules

When it comes to understanding the sugar hydrogenation mechanism, the question about which of the sugar tautomers are involved in the hydrogenation reaction remains to be answered, as there have been differing opinions regarding this

matter. Catalytic hydrogenation of D-fructose has been suggested to proceed via a closed ring formation[25,26,56] with some authors proposing the formation of α-fructofuranose.[57] However, there is also some more general information suggesting that hydrogenation of sugars proceeds via an open-chain formation.[8,12]

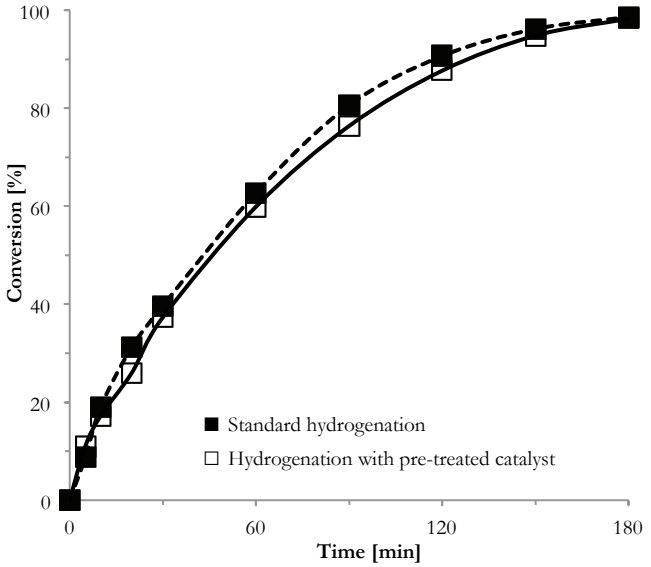

Figure 3.17. Effect of ultrasonic pre-treatment. D-galactose 4 %, 105 °C and 50 bar.

Furthermore, there have been several attempts at finding a mechanistically sound expression that describes the sugar hydrogenation. For the most common cases of D-glucose, D-lactose and D-xylose, it is possible to find studies and reviews that offer different ways of treating the reaction kinetics.[11,31,33,35,36,44,51,58,59] In the majority of these studies, the surface reactions are claimed to proceed via a Langmuir-Hinshelwood mechanism. However, there are differing opinions regarding the way hydrogen is adsorbed on the surface (molecularly or atomically) and regarding the occupation of active sites by hydrogen and the sugar molecule: (a) sugar and hydrogen compete for adsorption on the same type of sites or (b) sugar and hydrogen adsorb on different sites due to structural differences. In this respect, it is also worth mentioning that, by coupling quantum calculations and classic kinetic studies, it is possible to determine the amount of sites required by each molecule in order to adsorb and react on an active metal cluster.[57,60,61]

Due to the abovementioned arguments, some rival hypotheses were compared in the derivation of the rate equations for the hydrogenation of L-arabinose,

D-galactose, D-maltose and L-rhamnose. Such models consisted of Langmuir-Hinshelwood with non-competitive (Equation (3.5)) and competitive adsorption (Equation (3.6)) of reactants, and a semi-empirical model, Equation (3.7). Molecular adsorption of hydrogen was assumed in all of the models.

$$r_1 = \frac{k \cdot K_S \cdot K_{H_2} \cdot [S] \cdot P_{H_2}}{\left(1 + K_{H_2} \cdot P_{H_2}\right) \cdot \left(1 + K_S \cdot [S] + K_{S_{OH}} \cdot [S_{OH}]\right)} \tag{3.5}$$

$$r_1 = \frac{k \cdot K_S \cdot K_{H_2} \cdot [S] \cdot P_{H_2}}{\left(1 + K_{H_2} \cdot P_{H_2} + K_S \cdot [S] + K_{S_{OH}} \cdot [S_{OH}]\right)^2} \tag{3.6}$$

$$r_1 = \frac{k \cdot K_S \cdot K_{H_2} \cdot [S] \cdot P_{H_2}}{\left(1 + K_{H_2} \cdot P_{H_2} + K_S \cdot [S] + K_{S_{OH}} \cdot [S_{OH}]\right)} \tag{3.7}$$

The coefficients of determination for the models are presented in Table 3.8. The coefficient of determination, calculated from Equation (3.8), compares the model performance with respect to the variance of all experimental points. The coefficients of determination vary between 0 and 100%. A good deterministic model describing the reaction kinetics should have a high coefficient of determination, typically exceeding 95-97%. At a first glance, all the models were comparable (Table 3.8).

$$R^2 = \left(1 - \frac{\sum_{i=1}^{n} \left(c_{experimental_i} - c_{model_i}\right)^2}{\sum_{i=1}^{n} \left(c_{experimental_i} - c_{mean}\right)^2}\right) \cdot 100\% \tag{3.8}$$

A sensitivity analysis was performed by evaluating the impact of each parameter on the objective function. This analysis revealed that not only the competitive Langmuir-Hinshelwood model (Equation (3.6)) had a relatively better agreement with the experimental data, but also it was shown that the majority of the estimated parameters had an important contribution to the overall model performance, thus leading to a better identifiability.

In general, the parameters of the best models were well identified. However, the determination of the rate parameters for the side reactions was a more difficult task. As was the case of D-maltose, in which the activation energy for the D-maltitol cleavage to yield D-sorbitol was rather poorly identified. Despite of these shortcomings, the model can satisfactorily describe the experimental data.

Table 3.8. Coefficients of determination for the studied models.

	Competitive L-H	Non-competitive L-H	Semi-empirical
L-arabinose	98.67	95.20	97.99
D-galactose	97.34	96.78	97.27
D-maltose	98.58	98.55	98.47
L-rhamnose	94.15	94.23	94.00

A more detailed account of the derivation of the models as well as details about the general methods employed for the parameter estimation of the aforementioned models are presented in **Publication I**.

The estimation results shown in Figure 3.18, demonstrate how the model describes the behavior of the L-arabinose hydrogenation, for different hydrogen pressures and temperatures; the modeling of D-galactose, displayed in Figure 3.19, was also successful.

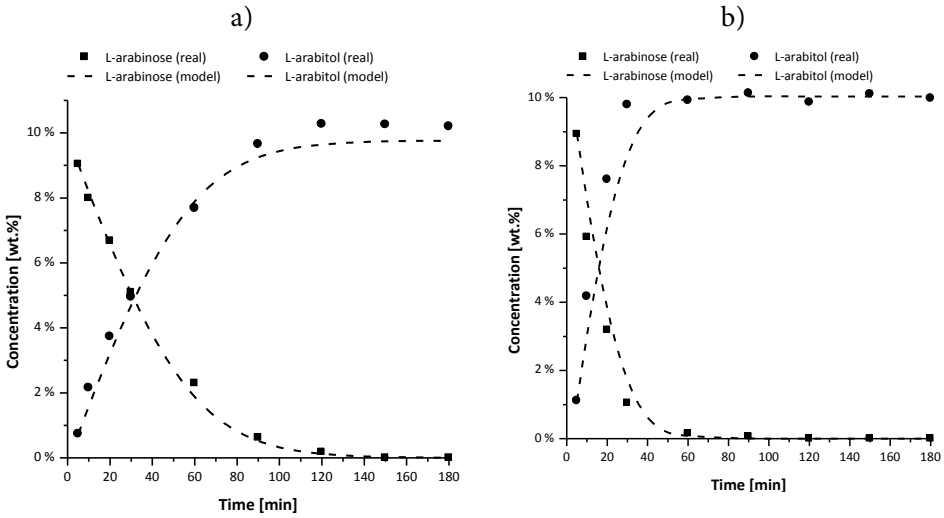

Figure 3.18. Modeling results for L-arabinose hydrogenation at different operation conditions: a) 105 °C and 50 bar and b) 120 °C and 60 bar.

The cases of L-rhamnose and D-maltose were somewhat different due to the existence of unidentified by-products, which had some negative impact on the quality of the model as shown in Figures 3.20 and 3.21, respectively.

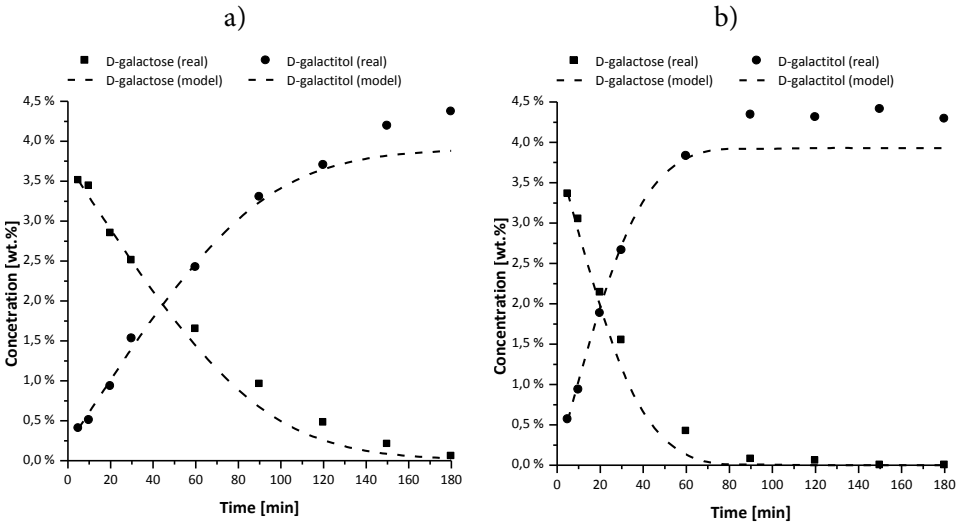

Figure 3.19. Modeling results for D-galactose hydrogenation at different operation conditions: a) 105 °C and 50 bar and b) 120 °C and 60 bar.

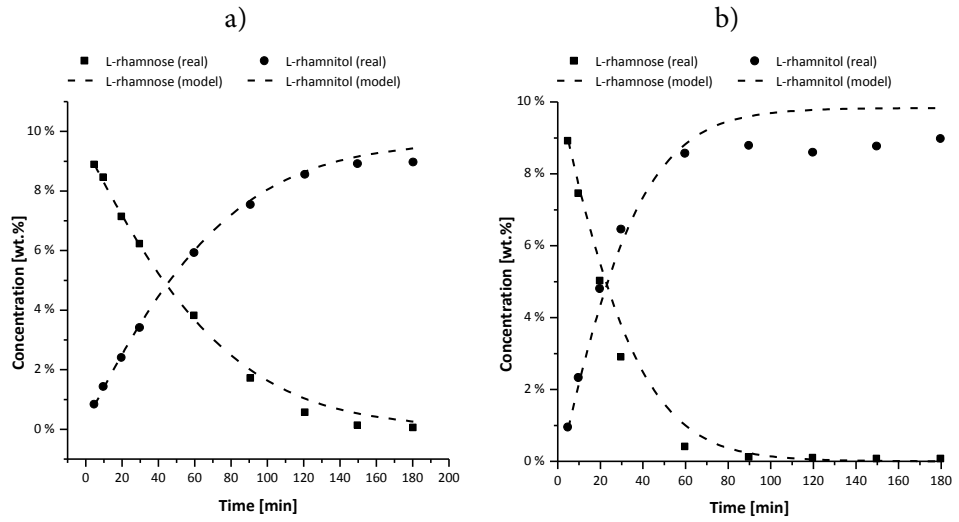

Figure 3.20. Modeling results for L-rhamnose hydrogenation at different operation conditions: a) 105 °C and 50 bar and b) 120 °C and 60 bar.

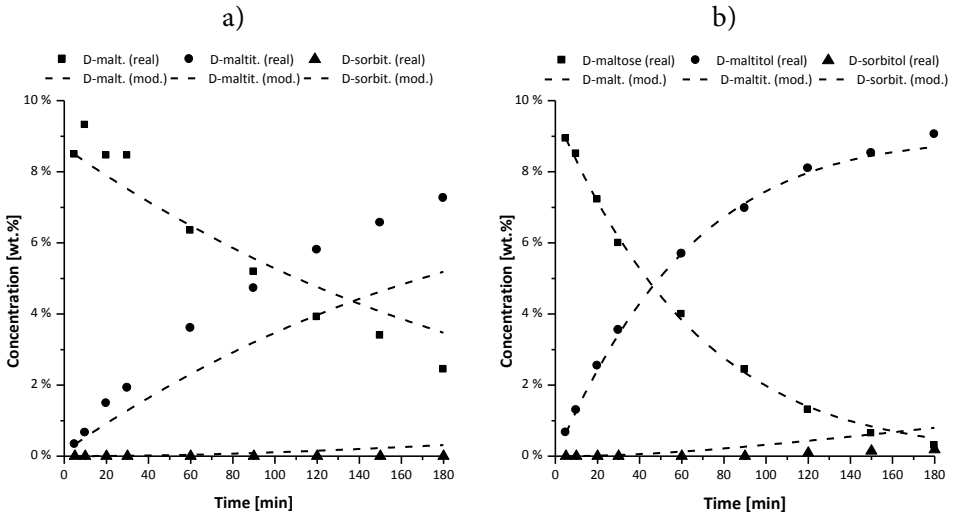

Figure 3.21. Modeling results for D-maltose hydrogenation at different operation conditions: a) 105 °C and 50 bar and b) 120 °C and 60 bar. Deviation of the maltitol concentration in Figure 3.21a might have been introduced by analytical errors.

3.8.2 Hydrogenation of mixtures

Starting from a Langmuir-Hinshelwood model that includes two kinds of active sites (one for hydrogen and another one for the sugars) and further neglecting product adsorption ($K_{A_{OH}}, K_{G_{OH}}$), we get Equations (3.9) and (3.10):

$$-r_A = \frac{k_1 \cdot K_{H2} \cdot K_A \cdot P_{H2} \cdot C_A}{(1 + K_{H2} \cdot P_{H2}) \cdot (1 + K_A \cdot C_A + K_G \cdot C_G)} \tag{3.9}$$

$$-r_G = \frac{k_2 \cdot K_{H2} \cdot K_G \cdot P_{H2} \cdot C_G}{(1 + K_{H2} \cdot P_{H2}) \cdot (1 + K_A \cdot C_A + K_G \cdot C_G)} \tag{3.10}$$

In case of a strong hydrogen adsorption, which is evidenced by the weak effect this parameter has in the overall reaction rate, we can perform the following simplification:

$$\lim_{K_{H2} \to strong} \frac{K_{H2} \cdot P_{H2}}{1 + K_{H2} \cdot P_{H2}} \to \frac{K_{H2} \cdot P_{H2}}{K_{H2} \cdot P_{H2}} = 1 \tag{3.11}$$

which leads to

$$-r_A = \frac{k'_1 \cdot C_A}{(1 + K_A \cdot C_A + K_G \cdot C_G)} \; ; \; k'_1 = k_1 \cdot K_A \tag{3.12}$$

$$-r_G = \frac{k'_2 \cdot C_G}{(1 + K_A \cdot C_A + K_G \cdot C_G)} \; ; \; k'_2 = k_2 \cdot K_G \tag{3.13}$$

Assuming that the adsorption on L-arabinose is stronger than that of D-galactose ($K_G \ll K_A$), as it will be proved in Section 3.8.3, we obtain:

$$-r_A = \frac{k'_1 \cdot C_A}{(1 + K_A \cdot C_A)} \tag{3.14}$$

$$-r_G = \frac{k'_2 \cdot C_G}{(1 + K_A \cdot C_A)} \tag{3.15}$$

The parameters yielded by the regression are summarized in Table 3.9 and exemplified by Figures 3.22 - 3.25. The fit of the model to the kinetic data is very good and the errors of the parameters are small, as revealed by the figures and the table.

Table 3.9. Parameter estimation results

Parameter	Est. params.	Est. rel. std. error (%)	Parameter	Est. params.	Est. rel. std. error (%)
E_{a_1}	49500.0	2.8	E_{a_2}	59600.0	1.6
A'^{*}_1	70.4	3.6	K_A	0.8	6.3
A'^{*}_2	39.0	1.8			

$^{*}k'_i = A'_i \cdot e^{-\left(\frac{E_{a_1}}{R \cdot T}\right)}$

The sensitivity analysis is a plot of the value of each estimated parameter against the corresponding objective function value, thus illustrating how well-defined these parameters are. A sharp valley indicates that the parameters are well-identified. This is illustrated for the activation energies for L-arabinose and D-galactose hydrogenation in Figures 3.26 and 3.27.

3.8.3 Product distribution analysis in sugar mixtures

A double logarithmic plot can further prove the correspondence of the studied process with the competitive Langmuir-Hinshelwood model proposed in Section 3.8.2. This method has been mostly applied to enzyme kinetics[62] and some catalytic mixture conversion of hydrocarbons[53,63] and it is based in the mathematical premise that the ratio of the conversion rates of two given components in the

mixture is proportional to the ratio of their concentrations. Consequently, if the mixture conversion satisfies the Langmuir-Hinshelwood model, a double logarithmic plot of the concentrations would produce a straight line.

Dividing Equation (3.9) by Equation (3.10) yields:

$$\frac{r_A}{r_G} = \frac{dC_A}{dC_G} = \frac{k_1 \cdot K_A \cdot [C_A]}{k_2 \cdot K_G \cdot [C_G]} \tag{3.16}$$

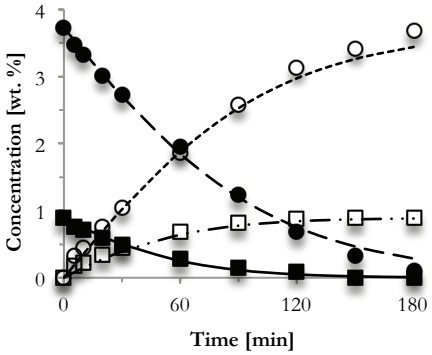

Figure 3.22. Modeling results at 105°C and 40 bar pressure. Ratio 3.6:1. ▪ L-arabinose, □ L-arabitol, ● D-galactose, ○ D-galactitol. Lines denote regression values.

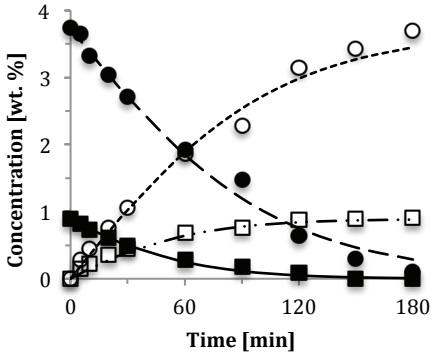

Figure 3.23. Modeling results at 105°C and 50 bar pressure. Ratio 3.6:1. . ▪ L-arabinose, □ L-arabitol, ● D-galactose, ○ D-galactitol. Lines denote regression values.

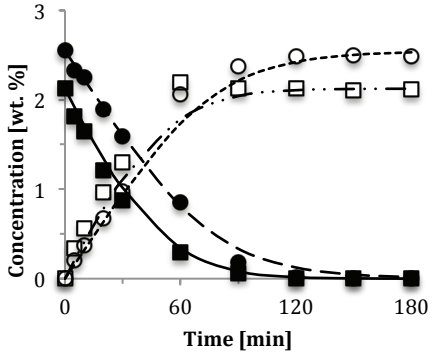

Figure 3.24. Modeling results at 120°C and 40 bar pressure. Ratio 1:1. ▪ L-arabinose, □ L-arabitol, ● D-galactose, ○ D-galactitol. Lines denote regression values.

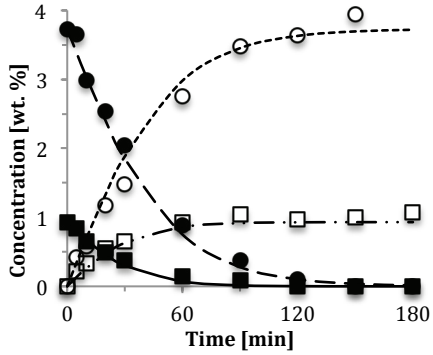

Figure 3.25. Modeling results at 120°C and 40 bar pressure. Ratio 3.6:1. ▪ L-arabinose, □ L-arabitol, ● D-galactose, ○ D-galactitol. Lines denote regression values.

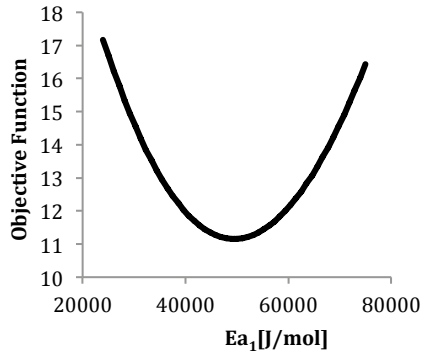

Figure 3.26. Sensitivity analysis for L-arabinose activation energy.

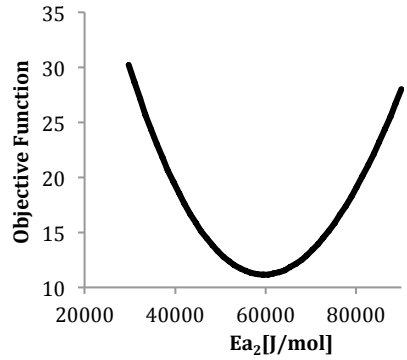

Figure 3.27. Sensitivity analysis for D-galactose activation energy.

This equation can be integrated between limits as,

$$\int_{C_{A,0}}^{C_A} \frac{dC_A}{C_A} = \alpha \cdot \int_{C_{G,0}}^{C_G} \frac{dC_G}{C_G} \; ; \; \alpha = \frac{k_1 \cdot K_A}{k_2 \cdot K_G} \tag{3.17}$$

where, $C_{A,0}$ and $C_{G,0}$ are the initial concentrations of L-arabinose and D-galactose, respectively. Performing the integration and inserting the integration limits gives,

$$ln\left(\frac{C_A}{C_{A,0}}\right) = \alpha \cdot ln\left(\frac{C_G}{C_{G,0}}\right) \tag{3.18}$$

α is the relative reactivity of L-arabinose to D-galactose and it remains constant during an isothermal experiment, if the mixture has an ideal behavior.

Since the only variables in equation are the sugar concentrations (C_A, C_G), the expression predicts a linear relation of $ln\left(\frac{C_A}{C_{A,0}}\right)$ as a function of $ln\left(\frac{C_G}{C_{G,0}}\right)$ and thus, from the slope of the plot, α can be evaluated. The double logarithmic plots from the performed experiments facilitate the analysis of the interaction between the two studied sugar species. From there, it can be deducted that both sugars follow the same kind of kinetics.

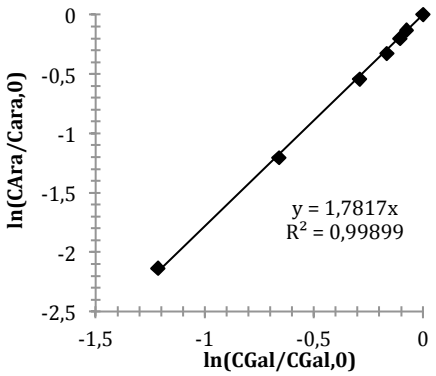

Figure 3.28. Hydrogenation of (D-gal:L-ara=0.5) solution at 120°C and 40 bar

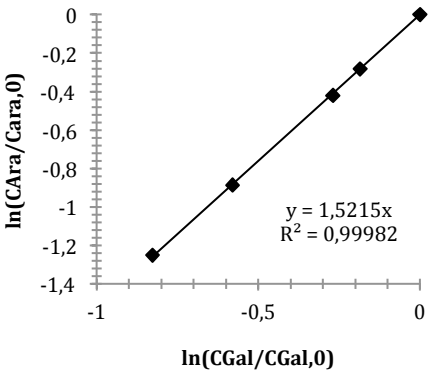

Figure 3.29. Hydrogenation of (D-gal:L-ara=5) solution at 120°C and 40 bar

As it can be gathered from Table 3.10, the relative reactivity of L-arabinose is always higher than that of D- galactose. The relative reactivity varies slightly with the initial composition, indicating, however, that the adsorption behavior of the system is not fully ideal.

A final test of the model was performed by preparing the first order plots of the conversion versus time data. Equation (3.18) relates the arabinose and galactose concentrations by:

$$\frac{c_A}{c_{A0}} = \left(\frac{c_G}{c_{G0}}\right)^{\alpha} \tag{3.19}$$

Table 3.10. Relative reactivities at different initial mole ratios.

n_{Gal}/n_{Ara}	α	n_{Gal}/n_{Ara}	α
0.1	1.73	**3.6**	1.63
0.5	1.78	**5.0**	1.52
1.0	1.83	**7.0**	1.47
2.0	1.70	**10**	1.41

The consumption rates of arabinose and galactose can now be written, according to Equations (3.14)-(3.15),

$$-r_A = \frac{k_1' \cdot c_A}{1 + K_A \cdot c_A} \tag{3.20}$$

$$-r_G = \frac{k_2' \cdot c_G}{1 + K_A \cdot c_{A0} \cdot \left(\frac{c_G}{c_{G0}}\right)^{\alpha}} \tag{3.21}$$

The concentrations are related to the conversions accordingly: $\left(\frac{c_A}{c_{A0}}\right) = 1 - X_A$ and $\left(\frac{c_G}{c_{G0}}\right) = 1 - X_G$. Since α is clearly larger than 1 (Table 3.10), the test plot for galactose should deviate more from linearity than the corresponding plot for arabinose. Figures 3.30 and 3.31 confirm that the plots are much more linear for L-arabinose than for D-galactose.

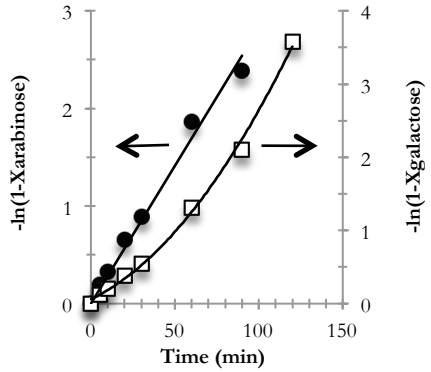

Figure 3.30. Hydrogenation of the Gal:Ara=3.6 solution at 120°C and 40 bar (X=conversion)

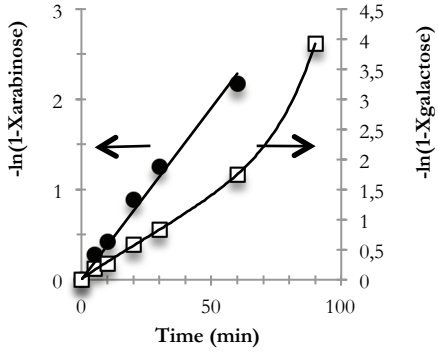

Figure 3.31. Hydrogenation of the Gal:Ara=5 solution at 120°C and 40 bar (X=conversion)

3.8.4 Hydrogenation inside a catalyst particle – interaction of reaction and diffusion

The porous catalyst particle was quantitatively described with a porous, reactive layer model including reaction, diffusion and catalyst deactivation. The model can be written as follows:

$$\frac{dc_i}{dt} = \varepsilon_p^{-1} \cdot \left(r_i \cdot \rho_p \cdot f(r) - r_\circ^s \cdot \frac{d(N_i \cdot r_\circ^s)}{dr_\circ} \right) \tag{3.22}$$

where the component generation rate (r_i) is calculated from the reaction stoichiometry,

$$r_i = \sum_j v_{ij} \cdot R_j \cdot a_j \tag{3.23}$$

c is the concentration, t is the reaction time, r is the length coordinate of the catalyst particle, ρ_p is the density of the catalyst particle and ε_p is the particle porosity. N is the molar flux, s is the shape factor (s=2 for spheres, s=1 for cylinders, s=0 for slabs), R_j is the rate of reaction j and a_j is the corresponding activity factor; (r) is the radial distribution function of the active sites: (r)=1.0 for conventional catalyst pellets but an increasing function for egg-shell catalysts. The form of the function can be determined experimentally with ICP-analysis and various mathematical functions can be fitted to the data, for instance $f = f_0 \cdot \left(\frac{r_\circ}{R_\circ}\right)^\alpha$.

The catalyst activity factor (a_j) is time-dependent. Several models have been proposed, depending on the origin of catalyst deactivation, i.e. sintering, fouling or poisoning. The following differential equation can represent semi-empirically different kinds of separable deactivation functions,

$$\frac{da_j}{dt} = -k_j'' \cdot \left(a_j - a_j^*\right)^n \tag{3.24}$$

where k_j'' is the deactivation parameter and a_j^* is the asymptotic value of the activity factor – for irreversible deactivation, $a_j^* = 0$. Depending on the value of the exponent (n), the solution of Equation (3.24) becomes

$$a_j = a_j^* + \left(a_{0j} - a_j^*\right) \cdot e^{-k_j'' \cdot t}, n = 1 \tag{3.25}$$

and

$$a_j = a_j^* + \left((a_o - a_*)^{1-n} + k_j'' \cdot (n-1) \cdot t\right)^{\frac{1}{1-n}}, n \neq 1 \tag{3.26}$$

Some special cases of Equation (3.25) are of interest: for irreversible first (n=1) and second (n=2) order deactivation kinetics we get $a_j = a_{0j} \cdot e^{-k_j'' \cdot t}$ and $a_j = \frac{a_{oj}}{1 + a_{oj} \cdot k_j'' \cdot t}$ respectively. The molar flux is given by $N_i = -D_{ei} \cdot \left(\frac{dc_i}{dr}\right)$, where $D_{ei} = \left(\frac{\varepsilon_p}{\tau_p}\right) \cdot D_{mi}$ according to the random pore model (D_{mi}= molecular diffusion

coefficient, D_{ei}= effective diffusion coefficient, ε_p/τ_p= particle porosity-to-tortuosity). A further development of Equation (3.22) yields:

$$\frac{dc_i}{dt} = \varepsilon_p^{-1} \cdot \left(\rho_p \cdot f(r) \cdot \sum v_{ij} \cdot R_j \cdot a_j + D_{ei} \cdot \left(\frac{d^2 c_i}{dr_\circ{}^2} + \frac{s}{r_\circ} \cdot \frac{dc_i}{dr_\circ} \right) \right) \tag{3.27}$$

The boundary conditions of Equation (3.27) are

$$\frac{dc_i}{dr_\circ} = 0 \tag{3.28}$$

at the particle center (r=0) and

$$c_i = c_i(R_\circ) \tag{3.29}$$

at the outer surface of the particle ($r_\circ = R_\circ$); c_i is the bulk concentration of the component. The initial condition at t=0 is ($r_\circ$)=c_i, i.e. equal to the bulk-phase concentration. The model was used to reveal the interaction between the intrinsic kinetics and diffusion in catalyst particles of different sizes [**Publication V**].

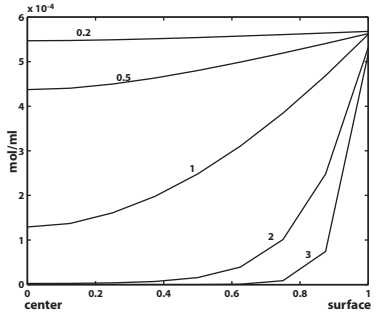

Figure 3.32. L-arabinose concentration profiles within catalyst particles of different sizes (mm) with an initial concentrations of 25 wt. % at 90°C.

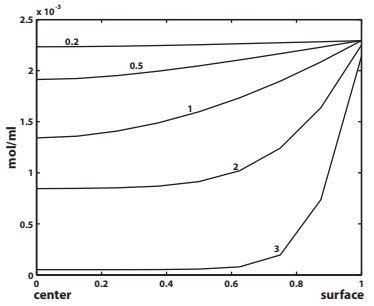

Figure 3.33. L-arabinose concentration profiles within catalyst particles of different sizes (mm) with an initial concentrations of 50 wt. % at 90 °C.

This approach provided fundamental information about kinetics coupled with mass-transfer phenomena and indicates that the sugar hydrogenation process should be carried out in slurry reactors or structured catalysts with thin catalyst layers to suppress diffusion resistance and to ensure high reaction rates (Figures 3.32 and 3.33, s=0). Moderate temperatures (100°C or less) are preferable to guarantee a high selectivity towards the desired products, the sugar alcohols.

3.8.5 Ultrasound and deactivation

In the quantitative description of the data obtained in the presence and absence of ultrasound, the main aim was to evaluate the ultrasound effect only. Thus, a very simple approach to kinetic modeling was taken.

A pseudo first order model with respect to the sugar and hydrogen was chosen to fit the data. This model was further optimized by the inclusion of an exponential deactivation term:

$$r_i = k_i \cdot C_A \cdot C_{H_2} \cdot e^{-k_j'' \cdot t_e} \tag{3.30}$$

with $k_i = A_i \cdot e^{-\frac{E_{a_i}}{R \cdot T}}$.

The values of parameters and model fitting are shown in Table 3.11.

Table 3.11. Parameter estimation overview

Sugar	Conditions	R^2	k_0	k_d
Galactose	Silent	97.54	4.60×10^{9} ±4.2 %	1.19×10^{-3} ±15.0 %
Galactose	US	95.50	6.50×10^{9} ±6.1 %	2.18×10^{-3} ±11.1 %
Arabinose	Silent	94.04	4.48×10^{7} ±6 %	1.32×10^{-3} ±19.3 %
Arabinose	US	97.68	4.33×10^{7} ±4.4	2.42×10^{-3} ±14.3

The pseudo-first order model was able to accurately describe the experiments carried out under silent conditions and gave reliable statistics. However, the model does not work very well in the case of the sonicated hydrogenation of L-arabinose (third experiment). Therefore, only the first and the second experiments were included in the parameter estimation of arabinose under sonicated conditions.

It can be concluded that the deactivation parameter (k_j'') obtained a higher value for sonicated experiments than for silent experiments. It should, however, be kept in mind that the parameters k_0 and k_j'' are to some extent numerically correlated.

3.8.6 Discussion on kinetic models

Three superficially different kinetic models were used in the present work. The model used for the kinetic study in **Publication I** (Equation (3.6)) was based on the principle of competitive adsorption of hydrogen and sugar molecules, while the model which was used to describe the kinetics of sugar mixtures in **Publication II** (Equation (3.5)) considered the adsorption of hydrogen and sugar molecules to be of non-competitive character, which can be justified by the big differences in the sizes of hydrogen and the sugar molecules. A very simple kinetic model was used to describe the interaction between the sugar hydrogenation kinetics and catalyst deactivation in **Publication III** (Equation (3.30)). The model used in **Publication III** can be obtained as a special case from the models presented in **Publications I** and **II** by neglecting the adsorption terms of the components.

It should be emphasized that it is in practice impossible to judge conclusively, based solely on kinetic studies, which model is the absolutely correct one. For instance, the data presented in **Publication I** were described quite well by the non-competitive adsorption model, too. The concept of non-competitive adsorption is, of course, a simplification, since some competition certainly takes place on the catalyst surface. In the work of Mikkola et al.[59], a physically more realistic semi-competitive adsorption model was introduced, which takes into account the size differences between the sugar molecules and hydrogen. This kind of model might be the best one for sugar hydrogenation, but its drawback is that an additional adjustable parameter is included to describe the size differences of the molecules. Separate adsorption studies and molecular modeling are needed to solve the issue of adsorption phenomena in sugar hydrogenation.

3.9 Continuous hydrogenation

3.9.1 Hydrogenation of L-arabinose with ACC and CSS supported Ru catalysts

The activity of the synthesized catalysts was tested according to the conditions illustrated in Table 2.1. The average conversions (i.e. the average of the discrete samples withdrawn at the outlet of the reactor throughout a time-on-stream of 150 minutes) and turnover numbers (TON) are summarized in Table 3.12.

Table 3.12. Catalyst performance

Catalyst	Average TON [moles L-ara/moles of surface Ru]	Avg. Conversion
ACC#1	147	17.9%
ACC#2	108	6.2%
ACC#3	236	7.3%
ACC#4	73	4.3%
CSS#1	0	0.0%
CSS#2	582	3.3%

In all the cases, except CSS#1, all the catalysts were active and, moreover, 100% selective towards L-arabitol as no by-products were detected by HPLC. The catalysts performances are represented in Figure 3.34. It must be noted that conversion is a direct result of, among others, the residence time, which can be adjusted by increasing the size of the catalyst bed.

The difference in the activity of the catalysts (TON) cannot be explained by the properties of the metal clusters as no clear trend could be established for the experiments carried on ACC/Ru catalysts. However, it was observed that CSS#2 exhibited a higher TON than its ACC counterparts but, in general, and considering the average conversion, ACC catalysts turned out to be superior to CSS catalysts.

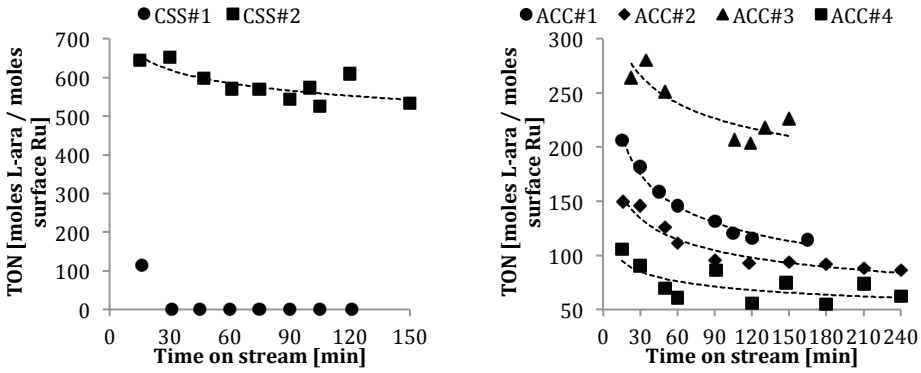

Figure 3.34. Catalyst performance

Regarding the endurance of the catalysts to deactivation under operating conditions, both catalyst groups exhibited a decrease in their activity during the first two hours of the experiments but once steady-state was reached and the apparent deactivation waned, the reactor reached a stable conversion rate.

3.9.2 Hydrogenation of L-arabinose with a commercial catalyst

A fractional factorial design of experiments was applied in order to assess the performance of the continuous hydrogenation system with the commercial catalyst extrudates (crushed). The studied parameters were temperature, gas flow, liquid flow and catalyst particle size and are summarized in Table 2.1 and Table 3.13.

As shown in Table 3.13, average conversions up to 13.7% were achieved. No by-products were observed. In the studied ranges, the temperature and liquid flow rate were the most determining factors, which becomes evident in both the average effect and in experiment #6.

The negative effect of both the gas and liquid flows suggests operation under sub-optimal residence times: at higher liquid rates, the residence time is at its shortest, which is further worsened by the entraining effect of the hydrogen flow. Increasing hydrogen flow evidently increased the gas hold-up and diminished the liquid hold-up, thus diminishing the liquid residence time, which impaired the conversion.

The positive effect of the temperature is tied to the increase of the reaction rate constant and increase of the hydrogen solubility with temperature.[49] However, it should be considered that sugars tend to decompose at higher temperatures, thus restricting the freedom at which the temperature can be manipulated.

Finally, it can be seen that the catalyst particle size had a minor effect under these circumstances. This is in correspondence with performed numerical calculations that suggest an optimal particle size of ca. 200 μm.[64] Moreover, the detrimental effect of the lower size fraction is related to the stability of the packed bed, as the smallest particles tend to be dragged along the flow thus slightly reducing the catalyst load. From this drawback, it becomes evident that structured catalysts in the form of Ru/ACC are to be preferred, as they exhibited a remarkable mechanical stability with no catalyst particles being transported downstream. In packed beds relevant for industrial conditions, the catalyst particle size should exceed 1 mm, which means that internal diffusion resistance becomes dominant (Section 0). For this reason, a structured catalyst also is preferable.

Table 3.13. Experimental grid for continuous L-arabinose hydrogenation*

Experiment	Temp. [°C]	H_2 flow [ml/min]	Liq. flow [ml/min]	Cat. part. size [µm]	Avg. conversion
1	+1	-1	+1	-1	4.81%
2	+1	+1	-1	-1	8.71%
3	+1	+1	+1	+1	3.54%
4	-1	-1	+1	+1	2.91%
5	-1	+1	+1	-1	3.43%
6	+1	-1	-1	+1	13.71%
7	-1	-1	-1	-1	8.21%
8	-1	+1	-1	+1	6.09%
Avg. effect	2.53%	-1.97%	-5.51%	0.28%	6.43%

**+1 indicates a high setting and -1 indicates a low setting. Refer to Table 2.1 for the corresponding values.*

4 Conclusions

The hydrogenation of D-maltose, D-galactose, L-arabinose and L-rhamnose as well as mixtures of L-arabinose and D-galactose on carbon-supported Ru catalyst in a pressurized slurry reactor was successfully performed: high conversions and selectivities towards the corresponding sugar alcohols were achieved without any significant by-product formation. Kinetic data were obtained under the conditions, in which intrinsic kinetics prevailed and the diffusion resistances were suppressed (small catalyst particles, low catalyst concentrations, high stirring speeds). The temperature effect on the reaction rate was strong, whereas the hydrogen pressure effect was minimal. Moderate temperatures (100 °C or less) are preferable to guarantee a high selectivity towards the desired products.

In the case of sugar mixtures, L-arabinose was more rapidly hydrogenated than D-galactose and it even exhibited a rate acceleration at the molar ratio 5:1 (L-arabinose:D-galactose) due to the interaction with the D-galactose hydrogenation. In this case, the hydrogenation mechanism obeyed a competitive behavior for the adsorption of both sugar molecules.

Regarding the implementation of ultrasound, it was observed that, in the range of power delivered through the indirect and direct methods (10-30W), favorable impact was observed for D-galactose but not for L-arabinose. However, and opposite to what was expected, intense exposition to ultrasound seems to intensify catalyst deactivation. Further analyses on the characterization of fresh and spent catalysis employed in conjunction with ultrasonic irradiation indicated that particle agglomeration occurred along with suspected poisoning due to iron leaching.

Hydrogenation of L-arabinose in a continuous three-phase reactor using different types of catalysts was successful. Deposition of Ru on ACC and CSS supports yielded active catalysts. Of these two supports, ACC proved to be superior as it is easily handled, structurally more stable than CSS and able to bond higher ruthenium loads.

A third, commercial catalyst was also employed for the purposes of screening different operational conditions. It was demonstrated that catalyst particles below 200 micrometers are indifferent to internal mass transfer and that L-arabinose hydrogenation thrives at relatively lower hydrogen and liquid flows, 100 ml/min and 1 ml/min respectively. Higher temperatures will yield an increased conversion but care should be taken in regards to the point at which sugar molecules start to undergo side reactions.

Physical properties of the four concerned sugars in aqueous solutions were studied (density, viscosity and hydrogen solubility). This data provides the primary information for the simulation of diverse process, including design and scale-up/number-up of hydrogenation reactors.

In terms of mathematical modeling, the first step was the advancement of a kinetic model that described well the experimental data of the conversion of single sugar molecules (L-arabinose, D-galactose, D-maltose and L-rhamnose) into sugar alcohols. Subsequently, a kinetic model was developed, which provided a good description of the hydrogenation of mixtures of L-arabinose and D-galactose.

Modeling of the catalyst deactivation kinetics under silent and sonicated conditions was carried out with a pseudo-first order model providing an acceptable fit for the hydrogenation of L-arabinose.

Reaction and diffusion modeling inside porous catalyst layers were made possible thanks to kinetic studies and modeling, and measurement of physical properties. This approach provided fundamental information about these phenomena and corroborated the requirement that efficient sugar hydrogenation processes be carried out in either slurry reactors or structured catalysts with thin catalyst layers in order to suppress diffusion resistance and to ensure high reaction rates.

Many paths have been opened as logical continuations to this research. Such as studies on molecular modeling, sugar isomerization kinetics and equilibria, as well as experiments on model catalysts with very well defined catalyst nanoparticle sizes to reveal any structure sensitivity. These tasks will ultimately provide the insight into the reaction mechanisms necessary to develop an even better Ru catalyst specially tailored for sugar hydrogenation.

Another area of opportunity regards the implementation and optimization of a continuous process, in which further development on structured supports, such as active carbon clothes and solid foams, as well as exploration of the possibilities of carbon nanotubes, are highly encouraged.

The ultimate goal should be integration of the sugar hydrogenation step into a biorefinery scheme, as envisioned in Figure 4.1. This requires that the homogeneous catalyst (typically mineral acid or organic acid) used in the hydrolysis of cellulose or hemicelluloses be separated from the mixture of sugar monomers before the hydrogenation step. This work has shown that it is possible to hydrogenate sugar monomer mixtures to complete conversion, but the solution should be free from dissolved acid catalysts to guarantee the activity of the solid hydrogenation catalyst.

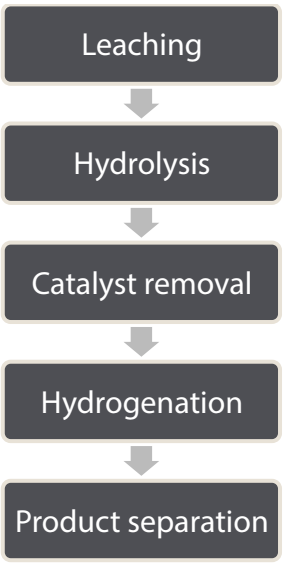

Figure 4.1. Biorefinery scheme

5 Notation

A'_i	Lumped pre-exponential factor
A_i	Pre-exponential factor
a_j	Catalyst activity factor
a_j^*	Asymptotic activity
A_{OH}	Arabitol
C_i	Concentration
C_i^*	Equilibrium concentration after step disturbance (gas solubility, Fugatron)
D_{ei}	Effective diffusion coefficient
D_{mi}	Molecular diffusion coefficient
E_{a_i}	Activation energy
f	Calibration constant in hydrogen solubility measurements
$f(r)$	Radial distribution function of active sites
G	Galactose
G_{OH}	Galactitol
H_2	Hydrogen
He	Henry's constant
K_i	Adsorption constant
k_i	Rate constant
k_i'	Lumped kinetic and adsorption constants
k_j''	Deactivation parameter
m_{cat}	Catalyst mass
n	Deactivation order
n_i	Amount of substance
N_i	Molar flux
P_i	Hydrogen pressure
R	Ideal gas constant
R^2	Coefficient of determination
r_j	Reaction rate of component i
R_j	Rate of reaction j

$r_\circ$	Particle length coordinate
$R_\circ$	Particle's length
s	Shape factor
T	Temperature
t	Time
t_e	Catalyst in-use time
V	Volume
X_i	Conversion of reactant i
α	Relative reactivity
ε_p	Particle porosity
θ_i	Catalyst site
μ	Viscosity
ν_0	Reference kinematic viscosity
ν_1	Kinematic viscosity of the sample
ρ	Density
ρ_B	Catalyst bulk density
ρ_p	Catalyst particle density
τ_p	Tortuosity
[ ]	Concentration

Subscripts

Gc	Carrier gas
L	Liquid phase
0	Initial state

Abbreviations

A	Arabinose
A_{OH}	Arabitol
G	D-Galactose
G_{OH}	Galactitol
H_2	Hydrogen
S	Sugar
S_{OH}	Sugar alcohol

6 References

[1] J. Sanders, E. Scott, R. Weusthuis, and H. Mooibroek, "Bio-refinery as the bio-inspired process to bulk chemicals," *Macromolecular Bioscience*, vol. 7, no. 2, pp. 105-17, Feb. 2007.

[2] D. M. Alonso, J. Q. Bond, and J. A. Dumesic, "Catalytic conversion of biomass to biofuels," *Green Chemistry*, vol. 12, no. 9, p. 1493, 2010.

[3] S. Murat Sen, C. A. Henao, D. J. Braden, J. A. Dumesic, and C. T. Maravelias, "Catalytic conversion of lignocellulosic biomass to fuels: Process development and technoeconomic evaluation," *Chemical Engineering Science*, vol. 67, no. 1, pp. 57-67, Jan. 2012.

[4] P. Gallezot, "Conversion of biomass to selected chemical products.," *Chemical Society reviews*, vol. 41, no. 4, pp. 1538-58, Feb. 2012.

[5] F. W. Lichtenthaler and S. Peters, "Carbohydrates as green raw materials for the chemical industry," *Comptes Rendus Chimie*, vol. 7, no. 2, pp. 65-90, Feb. 2004.

[6] R. R. Davda, J. W. Shabaker, G. W. Huber, R. D. Cortright, and J. A. Dumesic, "A review of catalytic issues and process conditions for renewable hydrogen and alkanes by aqueous-phase reforming of oxygenated hydrocarbons over supported metal catalysts," *Applied Catalysis B: Environmental*, vol. 56, no. 1–2, pp. 171-186, Mar. 2005.

[7] IUPAC, *Compendium of Chemical Terminology*, 2nd ed. Oxford: Blackwell Scientific Publications.

[8] P. Collins and R. Ferrier, *Monosaccharides: their chemistry and their roles in natural products*, 1st ed. Chichester; New York: Wiley & Sons, 1995, p. xix, 574 p.

[9] B. G. Davis and A. J. Fairbanks, *Carbohydrate Chemistry*. Oxford: Oxford University Press, 2002, p. 96.

[10] A. Corma, S. Iborra, and A. Velty, "Chemical routes for the transformation of biomass into chemicals.," *Chemical Reviews*, vol. 107, no. 6, pp. 2411-502, Jun. 2007.

[11] N. Déchamp, A. Gamez, A. Perrard, and P. Gallezot, "Kinetics of glucose hydrogenation in a trickle-bed reactor," *Catalysis Today*, vol. 24, no. 1–2, pp. 29-34, Jun. 1995.

[12] H. Li, H. Li, and J.-F. Deng, "Glucose hydrogenation over Ni–B/SiO2 amorphous alloy catalyst and the promoting effect of metal dopants," *Catalysis Today*, vol. 74, no. 1–2, pp. 53-63, May 2002.

[13] M. L. Cunningham and C. B. Walker, "Maltitol-rich solutions and their manufacture," Patent US 20040222004.

[14] M. Niimi, Y. Hario, Y. Ishii, K. Kataura, and K. Kato, "Preparation of maltose and maltitol from starch," Patent JP 02042991990.

[15] G. Darsow, "Preparation of epimer-free sugar alcohols," Patent EP 4235251991.

[16] M. Magara, K. Shimazu, M. Fuse, K. Kataura, J. Osada, K. Kato, and K. Yoritomi, "Manufacture of maltitol with high purity," Patent JP 010935971989.

[17] J. Kondo, T. Miyamoto, and M. Asano, "Maltitol from maltose," Patent JP 53119811978.

[18] A. Maisin, A. Lefèvre, A. Germain, and M. Wauters, "Reactivation of a catalyst containing platinum group metals for hydrogenation of sugars," Patent BE 8822791980.

[19] V. Benessere, R. Del Litto, A. De Roma, and F. Ruffo, "Carbohydrates as building blocks of privileged ligands," *Coordination Chemistry Reviews*, vol. 254, no. 5–6, pp. 390-401, Mar. 2010.

[20] G. Helmchen and C. Murmann, "Preparation of optically active diphosphine ligands as asymmetric hydrogenation cocatalyst," Patent EP 8858971998.

[21] V. B. Duffy and M. Sigman-Grant, "Position of the American Dietetic Association: use of nutritive and nonnutritive sweeteners.," *Journal of the American Dietetic Association*, vol. 104, no. 2, pp. 255-75, Feb. 2004.

[22] G. Livesey, "Glycaemic Responses and Toleration," in *Sweeteners and sugar alternatives in food technology*, H. Mitchell, Ed. Oxford ; Ames, Iowa: Blackwell Pub., 2006, pp. 3-18.

[23] C. Eisenbeis, R. Guettel, U. Kunz, and T. Turek, "Monolith loop reactor for hydrogenation of glucose," *Catalysis Today*, vol. 147S, p. S342-S346, Sep. 2009.

[24] J. Wisniak, M. Hershkowitz, R. Leibowitz, and S. Stein, "Hydrogenation of xylose to xylitol," *Industrial & Engineering Chemistry Product Research and Development*, vol. 13, no. 1, pp. 75–79, Dec. 1974.

[25] A. W. Heinen, J. A. Peters, and H. van Bekkum, "Hydrogenation of fructose on Ru/C catalysts," *Carbohydrate Research*, vol. 328, no. 4, pp. 449-457, Oct. 2000.

[26] M. Makkee, A. P. G. Kieboom, and H. van Bekkum, "Hydrogenation of D-fructose and D-fructose D-glucose mixtures," *Carbohydrate Research*, vol. 138, no. 2, pp. 225-236, 1985.

[27] B. Chen, U. Dingerdissen, J. G. E. Krauter, H. Lansinkrotgerink, K. Mobus, D. J. Ostgard, P. Panster, T. H. Riermeier, S. Seebald, T. Tacke, H. Rotgerink, and H. Trauthwein, "New developments in hydrogenation catalysis particularly in synthesis of fine and intermediate chemicals," *Applied Catalysis, A: General*, vol. 280, no. 1, pp. 17-46, Feb. 2005.

[28] J. Kuusisto, J.-P. Mikkola, M. Sparv, J. Wärnå, H. Heikkilä, R. Perälä, J. Väyrynen, and T. Salmi, "Hydrogenation of Lactose over Sponge Nickel Catalysts - Kinetics and Modeling," *Industrial & Engineering Chemistry Research*, vol. 45, no. 17, pp. 5900-5910, Aug. 2006.

[29] J.-P. Mikkola, R. Sjöholm, T. Salmi, and P. Mäki-Arvela, "Xylose hydrogenation: kinetic and NMR studies of the reaction mechanisms," *Catalysis Today*, vol. 48, no. 1–4, pp. 73-81, Jan. 1999.

[30] E. Crezee, B. W. Hoffer, R. J. Berger, M. Makkee, F. Kapteijn, and J. A. Moulijn, "Three-phase hydrogenation of D-glucose over a carbon supported ruthenium catalyst-mass transfer and kinetics," *Applied Catalysis, A: General*, vol. 251, pp. 1-17 ST - Three-phase hydrogenation of D-glucose, 2003.

[31] J. Wisniak and R. Simon, "Hydrogenation of glucose, fructose, and their mixtures," *Industrial & Engineering Chemistry Product Research and Development*, vol. 18, no. 1, pp. 50–57, 1979.

[32] IARC, "Chromium, nickel and welding.," *IARC monographs on the evaluation of carcinogenic risks to humans / World Health Organization, International Agency for Research on Cancer*, vol. 49, pp. 1-648, Jan. 1990.

[33] E. Crezee, B. W. Hoffer, R. J. Berger, M. Makkee, F. Kapteijn, and J. A. Moulijn, "Three-phase hydrogenation of D-glucose over a carbon supported ruthenium catalyst—mass transfer and kinetics," *Applied Catalysis, A: General*, vol. 251, no. 1, pp. 1-17, Sep. 2003.

[34] J.-P. Mikkola, T. Salmi, and R. Sjöholm, "Effects of solvent polarity on the hydrogenation of xylose," *Journal of Chemical Technology and Biotechnology*, vol. 76, no. 1, pp. 90-100, Jan. 2001.

[35] J. Kuusisto, J.-P. Mikkola, M. Sparv, J. Warna, H. Karhu, and T. Salmi, "Kinetics of the catalytic hydrogenation of D-lactose on a carbon supported ruthenium catalyst," *Chemical Engineering Journal*, vol. 139, no. 1, pp. 69-77, May 2008.

[36] J. Kuusisto, J.-P. Mikkola, P. Casal, H. Karhu, J. Vayrynen, and T. Salmi, "Kinetics of the catalytic hydrogenation of D-fructose over a CuO-ZnO catalyst," *Chemical Engineering Journal*, vol. 115, no. 1–2, pp. 93-102, Dec. 2005.

[37] T. Salmi, J. Kuusisto, J. Wärnå, and J.-P. Mikkola, "Alternative sweeteners: la dolce vita," *Chimica e l'Industria (Milan, Italy)*, vol. 88, no. 8, pp. 90-96, 2006.

[38] T. O. Salmi, D. Y. Murzin, J. P. Wärnå, J.-P. Mikkola, J. E. B. Aumo, and J. Kuusisto, "Modeling and Optimization of Complex Three-Phase Hydrogenations and Isomerizations under Mass-Transfer Limitation and Catalyst Deactivation," in *Catalysis of Organic Reactions*, vol. 115, S. Schmidt, Ed. CRC Press, 2006, pp. 187-196.

[39] J.-P. Mikkola and T. Salmi, "In-situ ultrasonic catalyst rejuvenation in three-phase hydrogenation of xylose," *Chemical Engineering Science*, vol. 54, no. 10, pp. 1583–1588, May 1999.

[40] B. Toukoniitty, E. Toukoniitty, P. Mäki-Arvela, J.-P. Mikkola, T. Salmi, D. Y. Murzin, and P. J. Kooyman, "Effect of ultrasound in enantioselective hydrogenation of 1-phenyl-1,2-propanedione: comparison of catalyst activation, solvents and supports.," *Ultrasonics Sonochemistry*, vol. 13, no. 1, pp. 68-75, Jan. 2006.

[41] B. Toukoniitty, J. Kuusisto, J. P. Mikkola, T. Salmi, and D. Y. Murzin, "Effect of ultrasound on catalytic hydrogenation of D-fructose to D-mannitol," *Industrial & Engineering Chemistry Research*, vol. 44, no. 25, pp. 9370–9375, 2005.

[42] B. Toukoniitty, E. Toukoniitty, J. Kuusisto, J.-P. Mikkola, T. Salmi, and D. Murzin, "Suppression of catalyst deactivation by means of acoustic irradiation — Application on fine and specialty chemicals," *Chemical Engineering Journal*, vol. 120, no. 1–2, pp. 91-98, Jul. 2006.

[43] B. Toukoniitty, J.-P. Mikkola, D. Y. Murzin, and T. Salmi, "Utilization of electromagnetic and acoustic irradiation in enhancing heterogeneous catalytic reactions," *Applied Catalysis, A: General*, vol. 279, no. 1–2, pp. 1-22, Jan. 2005.

[44] J. Wisniak, M. Hershkowitz, and S. Stein, "Hydrogenation of Xylose over Platinum Group Catalysts," *Industrial & Engineering Chemistry Product Research and Development*, vol. 13, no. 4, pp. 232-236, Dec. 1974.

[45] P. J. Simms, K. B. Hicks, R. M. Haines, A. T. Hotchkiss Jr., and S. F. Osman, "Separation of lactose, lactobionic acid and lactobionolactone by high-

performance liquid chromatography," *Journal of Chromatography A*, vol. 667, no. 1–2, pp. 67-73, Apr. 1994.

[46] A. Weissler, H. W. H. W. Cooper, and S. Snyder, "Chemical Effect of Ultrasonic Waves: Oxidation of Potassium Iodide Solution by Carbon Tetrachloride," *Journal of the American Chemical Society*, vol. 72, no. 4, pp. 1769-1775, 1950.

[47] D. R. Lide, Ed., *CRC Handbook of Chemistry and Physics*, 89th ed. CRC Press, 2008, p. 2736.

[48] M. Meyberg and F. Roessler, "In Situ Measurement of Steady-State Hydrogen Concentrations during a Hydrogenation Reaction in a Gas-Inducing Stirred Slurry Reactor," *Industrial & Engineering Chemistry Research*, vol. 44, no. 25, pp. 9705-9711, Dec. 2005.

[49] V. A. Sifontes Herrera, O. Oladele, K. Kordás, K. Eränen, J.-P. Mikkola, D. Y. Murzin, and T. Salmi, "Sugar hydrogenation over a Ru/C catalyst," *Journal of Chemical Technology and Biotechnology*, vol. 86, no. 5, pp. 658-668, May 2011.

[50] M. Migliori, D. Gabriele, R. Di Sanzo, B. de Cindio, and S. Correra, "Viscosity of multicomponent solutions of simple and complex sugars in water," *Journal of Chemical & Engineering Data*, vol. 52, no. 4, pp. 1347-1353, Jul. 2007.

[51] P. H. Brahme and L. K. Doraiswamy, "Modeling of a slurry reaction - hydrogenation of glucose on raney-nickel," *Industrial & Engineering Chemistry Process Design and Development*, vol. 15, no. 1, pp. 130-137, Jan. 1976.

[52] B. T. Kusema, G. Hilpmann, P. Mäki-Arvela, S. Willför, B. Holmbom, T. Salmi, and D. Y. Murzin, "Selective Hydrolysis of Arabinogalactan into Arabinose and Galactose Over Heterogeneous Catalysts," *Catalysis Letters*, vol. 141, no. 3, pp. 408-412, Dec. 2010.

[53] Y. I. Pyatnitsky, "Some new approaches to the competitive catalytic reaction kinetics," *Applied Catalysis, A: General*, vol. 113, no. 1, pp. 9-28, Jun. 1994.

[54] K. J. Moulton, S. Koritala, and E. N. Frankel, "Ultrasonic hydrogenation of soybean oil," *Journal of the American Oil Chemists' Society*, vol. 60, no. 7, pp. 1257-1258, Jul. 1983.

[55] K. J. Moulton, S. Koritala, K. Warner, and E. N. Frankel, "Continuous ultrasonic hydrogenation of soybean oil. II. Operating conditions and oil quality," *Journal of the American Oil Chemists' Society*, vol. 64, no. 4, pp. 542-547, Apr. 1987.

[56] J. F. Ruddlesden, A. Stewart, D. J. Thompson, and R. Whelan, "Diastereoselective control in ketose hydrogenations with supported copper and nickel-catalysts," *Faraday Discuss.*, vol. 72, pp. 397-411, 1981.

[57] D. J. Ostgard, V. Duprez, M. Berweiler, S. Röder, and T. Tacke, "Science and Technology in Catalysis 2006 : proceedings of the fifth Tokyo conference on advanced catalytic science and technology, Tokyo, July 23-28, 2006," in *Studies in surface and catalysis*, K. Eguchi, M. Machida, and I. A. N.-001480978 Yamanaka, Eds. Amsterdam: Elsevier Science Ltd, 2007, p. xxvii, 631 p.

[58] F. Turek, R. K. K. Chakrabarti, R. Lange, R. Geike, and W. Flock, "On the experimental study and scale-up of three-phase catalytic reactors: Hydrogenation of glucose on nickel catalyst," *Chemical Engineering Science*, vol. 38, no. 2, pp. 275-283, Jan. 1983.

[59] J.-P. Mikkola, T. Salmi, and R. Sjöholm, "Modelling of kinetics and mass transfer in the hydrogenation of xylose over Raney nickel catalyst," *Journal of Chemical Technology and Biotechnology*, vol. 74, no. 7, pp. 655-662, Jul. 1999.

[60] M. C. M. C. Castoldi, L. D. T. D. T. Câmara, R. S. S. Monteiro, A. M. M. Constantino, L. Camacho, J. W. D. Carneiro, D. A. G. Aranda, and J. W. M. de Carneiro, "Experimental and theoretical studies on glucose hydrogenation to produce sorbitol," *Reaction Kinetics and Catalysis Letters*, vol. 91, no. 2, pp. 341-352, 2007.

[61] H. Bernas, A. Taskinen, J. Wärnå, and D. Y. Murzin, "Describing the inverse dependence of hydrogen pressure by multi-site adsorption of the reactant:

Hydrogenolysis of hydroxymatairesinol on a Pd/C catalyst," *Journal of Molecular Catalysis A: Chemical*, vol. 306, no. 1–2, pp. 33-39, Jul. 2009.

[62] M. Baboshin and L. Golovleva, "Multisubstrate kinetics of PAH mixture biodegradation: analysis in the double-logarithmic plot.," *Biodegradation*, vol. 22, no. 1, pp. 13-23, Feb. 2011.

[63] C. P. Rader and H. A. Smith, "Competitive Catalytic Hydrogenation of Benzene, Toluene and the Polymethylbenzenes on Platinum," *Journal of the American Chemical Society*, vol. 84, no. 8, pp. 1443-1449, 1962.

[64] V. A. Sifontes, D. Rivero, J. P. Wärnå, J.-P. Mikkola, and T. O. Salmi, "Sugar Hydrogenation Over Supported Ru/C — Kinetics and Physical Properties," *Topics in Catalysis*, vol. 53, no. 15–18, pp. 1278-1281, May 2010.

ISBN 978-952-12-2731-8